Conic Optimization of Electric Power Systems

by

Joshua Adam Taylor

B.S., Carnegie Mellon University (2006)
S.M., Massachusetts Institute of Technology (2008)

Submitted to the Department of Mechanical Engineering
in partial fulfillment of the requirements for the degree of

Doctor of Philosophy

at the

MASSACHUSETTS INSTITUTE OF TECHNOLOGY

June 2011

Author .....
Department of Mechanical Engineering
June 2, 2011

Certified by .....
Franz S. Hover
Finmeccanica Career Development Professor of Engineering
Thesis Supervisor

Accepted by .....
David E. Hardt
Chairman, Department Committee on Graduate Students

Conic Optimization of Electric Power Systems

by

Joshua Adam Taylor

Submitted to the Department of Mechanical Engineering
on May 1, 2011, in partial fulfillment of the
requirements for the degree of
Doctor of Philosophy

Abstract

The electric power grid is recognized as an essential modern infrastructure that poses numerous canonical design and operational problems. Perhaps most critically, the inherently large scale of the power grid and similar systems necessitates fast algorithms. A particular complication distinguishing problems in power systems from those arising in other large infrastructures is the mathematical description of alternating current power flow: it is nonconvex, and thus excludes power systems from many frameworks benefiting from theoretically and practically efficient algorithms. However, advances over the past twenty years in optimization have led to broader classes possessing such algorithms, as well as procedures for transferring nonconvex problem to these classes.

In this thesis, we approximate difficult problems in power systems with tractable, conic programs. First, we formulate a new type of NP-hard graph cut arising from undirected multicommodity flow networks. An eigenvalue bound in the form of the Cheeger inequality is proven, which serves as a starting point for deriving semidefinite relaxations. We next apply a lift-and-project type relaxation to transmission system planning. The approach unifies and improves upon existing models based on the DC power flow approximation, and yields new mixed-integer linear, second-order cone, and semidefinite models for the AC case. The AC models are particularly applicable to scenarios in which the DC approximation is not justified, such as the all-electric ship. Lastly, we consider distribution system reconfiguration. By making physically motivated simplifications to the *DistFlow* equations, we obtain mixed-integer quadratic, quadratically constrained, and second-order cone formulations, which are accurate and efficient enough for near-optimal, real-time application.

We test each model on standard benchmark problems, as well as a new benchmark abstracted from a notional shipboard power system. The models accurately approximate the original formulations, while demonstrating the scalability required for application to realistic systems. Collectively, the models provide tangible new tradeoffs between computational efficiency and accuracy for fundamental problems in power systems.

Thesis Supervisor: Franz S. Hover
Title: Finmeccanica Career Development Professor of Engineering

Acknowledgments

As a student in the ocean area of a mechanical engineering department working on terrestrial power systems, it was tempting to make the title of this thesis something like 'fighting the current' or 'against the flow'; yet, I could not have imagined a better course to have taken through graduate school, and this is largely due to the people who accompanied me along the way. First, an enormous thanks to my advisor, Professor Franz Hover, who taught me (among many things) never fear to apply my own creativity, and who has also become a close friend.

I'd like to thank my committee, Professors Jim Kirtley, Sanjay Sarma, and John Tsitsiklis for their thoughtful guidance and advice over the past two years. A large portion of Chapter 3 benefited from discussions with Professor Daniel Stroock when I was stuck. Dr. Julie Chalfant deserves special thanks for helping me formulate the example in Section 4.6.4.

Over the past five years, I've been privileged to wonderful friends, without whom this experience would not have been what it was. As a member of the Hovergroup, I've had the pleasure of daily interaction with a number of smart and interesting people, all of whom I'd like to acknowledge, but especially Matt Greytak and Brendan Englot; I hope that we can continue our conversations in the future, if perhaps from different fields. The game of squash has been an essential outlet for me, and it will be difficult if not impossible to find substitutes for my weekly matches with Woradorn Wattanapanitch and Arup Chakraborty, as well as the rest of the MIT squash community. I feel truly lucky to have been been through some unforgettably fun times with a very cohesive circle of friends: my two amigos, Austin Minnich and Allison Beese, Matthew Branham, Eerik Hantsoo, Priam Pillai, Erica Ueda, and Kit Werley. And, because he requested it, but also because he's been my best friend for many years, Daniel Muenz gets mentioned now.

Every year I realize more and more what an incredible family I have, and how much they have shaped who I am. Stuart and Sheila, Rachel and David: this thesis is dedicated to you.

Support is acknowledged from the Office of Naval Research, Grant N00014-02-1-0623.

Contents

List of Figures

Chapter 1

Introduction

1.1 Motivation

The electric power grid is an integral part of all modern societies. Since the first public electricity supply was constructed in 1881 in Godalming, England, the power grid has steadily grown to accommodate continually increasing usage of electric power; consumption in the United States went from roughly four to forty quadrillion Btu from 1949 to 2009 [3].

A critical debate of the late 1880's was the so-called 'war of the currents' between Thomas Edison, who advocated direct current, and George Westinghouse, a proponent of the alternating current technology developed by Nicola Tesla [74]. The winning argument was that it was much easier using available technologies to change voltage levels with AC, permitting flexibility between high voltage transmission and lower voltage generation and end usage. Part of Edison's opposition to and initial dismissal of AC transmission was rooted in the higher level of mathematics necessary to understand it, which was not accessible to him. Basic AC power flow is however relatively easy to model with complex arithmetic and differential equations; yet, as will be seen in this thesis, many modern problems in power systems that would be straightforward to analyze in the DC case are in fact quite difficult due to the complexity of the resulting equations in the AC case.

Many of the problems made difficult by the presence of AC power flow terms

are at the system level, containing information about generation, loads, and their interconnections. While already difficult to analyze in simple two-bus cases, system-level descriptions typically involve large, networked systems of equations, further compounding the difficulty. Simply finding the power flow for a given operating condition, arguably the most fundamental system-level task in power systems, is complicated by convergence of standard algorithms to non-physical solutions [124]. The same basic power flow, in varying forms, is a central component of almost all more detailed problems, many of which have existed since the inception of the grid, and yet remain core to modern problems. Consider, for example, the following. Microgrids, small, potentially autonomous power systems sustained by local generation, have introduced new stability issues [79], which are often additionally challenging because of the fact that many microgrids will have distributed or renewable generation, much of which is inherently intermittent [102]. Stability, a canonical problem in its own right, must of course include information about power flow [83]. A second example is deregulation [109], which has introduced economic objectives in power flow, changing how generation is selected [126], and consequently necessitating new approaches to transmission planning [49]. Lastly, next generation naval ships will be largely electric, and will have unique generation and loading profiles for which new approaches to both stability and distribution design will be needed [44, 128].

As the size of and number of interconnections in power systems continues to grow, it has become increasingly apparent that not only are system-level problems such as those indicated above present, but that their consideration is essential to truly designing and operating for realistic scenarios. The specific justification for system-level modeling and the motivation behind this work are rooted in two contexts: the modern electric grid and the all-electric ship. In addition to most operational objectives being global functions, e.g. resistive losses, system-wide phenomena like instability and blackouts [8] have made apparent the fact that local design and operation are not adequate, particularly in the presence of economic factors [91]. Similarly, tightly coupled physics necessitate system-level approaches if efficient operation is to be achieved for the all-electric ship [26, 47, 128].

Many system-level problems like those discussed above can be posed as optimizations; indeed, the first minimum spanning tree algorithm was developed for the purpose of designing an electrical network in Moravia [23,24]. Now a variety of such problems exist, such as transmission system planning and distribution system reconfiguration, two subjects of this thesis. The main computational difficulty with the associated optimization problems are that they are large, and large problems simply take longer to solve. Additional difficulties in power system problems are caused by discreteness and nonconvexity, each of which is a manifestation of the curse of dimensionality [15]. The size of and presence of discrete quantities in power systems is shared across a number of modern infrastructures in which optimization plays a large role, for example transportation and communication networks. A distinction arises from the nonconvex mathematical description of AC power flow; *it is the goal of this thesis to identify and apply the most suitable tools available for ameliorating this aspect, transforming intractable problems into ones amenable to conventional mathematical programming tools.*

Mathematical programming approaches to power systems problems came to prominence in the 1960's and 1970's, primarily in the context of designing transmission networks [57] and power flows [45]. Tools available at the time restricted models to either efficient but highly simplified linear programs or descriptive but inefficient nonlinear programs. This development proceeded until the 1990's, when heuristic methods gained popularity for their ability to treat complicated optimization problems as "black boxes" [80,127]. On problems with nice properties, however, heuristics exhibit much slower convergence than classical algorithms because much of the available information is never utilized. There are indeed many nice properties to be exploited in power system optimization problems. There has furthermore been significant progress over the past twenty years in convex optimization, namely conic optimization methods such as second-order cone and semidefinite programming [25,93,118], as well as in systematic procedures for approximating nonconvex problems as conic programs with adjustable accuracy [85,101,111]. We apply a subset of these tools and obtain efficient new approaches which are applicable to longstanding existing problems, as

well as newer problems built upon older frameworks such as those discussed here.

In this work, a practical viewpoint is adopted in which tractability is associated with existence of mature, efficient software tools; for example, although NP-hard, we consider mixed-integer linear programming an 'easy' framework to solve problems within due to the efficacy of standard algorithms [108]. Thus, each portion of this thesis in some way concerns transforming a difficult, large optimization problem into one amenable to established methods.

1.2 Overview and contributions

Chapter 2 is intended to provide background relevant to the contributions of this work. First, models of AC power flow are summarized, as well as the DC power flow simplification. We discuss conic optimization and why it is effective, followed by a brief description and two examples of lift-and-project relaxations. A literature review is then given for the three areas of contribution, after which we are able to provide a unified description of the thesis.

In Chapter 3, we extend the Cheeger inequality of spectral graph theory to multicommodity flow networks. The result is used to construct semidefinite lift-and-project relaxations for a multicommodity flow network version of the Cheeger constant, which is a generalization of the sparsest cut. We then discuss as a potential application the use of matrix perturbation theory to estimate the probability a single-commodity flow network is feasible.

In Chapter 4, we address transmission system planning. First, prior work on linearized DC models is summarized and framed in terms of lift-and-project relaxations, following which the same viewpoint is applied to the AC case. The result is a spectrum of linear models based on the DC approximation, and an entirely new set of models for the full AC case, which had previously only been handled using full nonlinear approaches and heuristics. Specific formulations pertaining to shipboard power systems are given near the end, followed by computational examples which include a new benchmark case abstracted from a notional shipboard power system.

Chapter 5 covers distribution system reconfiguration. An efficient, mixed-integer quadratic model is formulated using the *simplified DistFlow* equations, and shown theoretically to produce radial configurations. Then, more accurate quadratically constrained and second-order cone approximations to the full *DistFlow* equations are derived, which once incorporated into the reconfiguration problem are able to accommodate a wider range of objectives. Under the loss minimization objective, the mixed-integer quadratic model is an order of magnitude faster than times reported in the literature.

We conclude in Chapter 6 by summarizing the contents of this thesis and identifying some venues for future research.

Chapter 2

Background

In this chapter, we provide brief technical foundations and literature reviews for the contributions of this thesis. Specifically,

- The technical material of Chapter 3 with the first part of the literature review is largely self-contained, but Sections 2.2 and 2.3 highlight common threads it shares with with Chapters 4 and 5.
- Sections 2.1, 2.2, and 2.3, as well as the second part of the literature review are used in developing new transmission planning models in Chapter 4.
- Sections 2.1 and 2.2 and the third part of the literature review form a basis for Chapter 5 on distribution system reconfiguration.

We conclude this chapter with a paragraph on the work's connecting themes and a comment on mixed-integer conic optimization.

2.1 Steady state power flow

As stated in the Introduction, a significant distinction between electric power systems, terrestrial and shipboard, and other large infrastructures is the nonlinear and moreover nonconvex dynamic description of AC power flow. In this section, we summarize the most popular formulations of AC power flow, all of which in general result

in nonconvex feasible sets when incorporated into optimizations with voltage variables [92]. We restrict our focus to the steady state, for which the complex equations for AC power flow are given by [124]

$$\begin{aligned} s_{ij} &= v_i v_i^* y_{ij}^* - v_i v_j^* y_{ij}^* \\ \sum_j s_{ij} &= s_i^L, \end{aligned} \tag{2.1}$$

where i and j are bus indices, v is complex bus voltage, y admittance, s power flow, and s^L the power generated or consumed at a bus. It is often convenient to separate (2.1) into real and imaginary parts; this can be done in two ways. In the polar formulation, the basic variables are the voltage magnitude and phase angle, while in the rectangular formulation voltage is expressed in terms of real and imaginary components:

$$v = |v|e^{j\theta} = w + jx. \tag{2.2}$$

Historically, the polar formulation has seen wider usage because it is a more convenient starting point for deriving approximations. It is written

$$\begin{aligned} p_{ij} &= g_{ij}|v_i|^2 - |v_i||v_j|\left(g_{ij}\cos(\theta_i - \theta_j) + b_{ij}\sin(\theta_i - \theta_j)\right) \\ q_{ij} &= -b_{ij}|v_i|^2 - |v_i||v_j|\left(g_{ij}\sin(\theta_i - \theta_j) - b_{ij}\cos(\theta_i - \theta_j)\right) \\ \sum_{j:i\sim j} p_{ij} &= p_i^L \\ \sum_{j:i\sim j} q_{ij} &= q_i^L \end{aligned} \tag{2.3}$$

where p and q are real and reactive power flows, p^L and q^L are real and reactive bus load and generation, and g and b are conductance and susceptance.

DC power flow [124], the most severe approximation one can make without going to network flow [4, 76], is obtained by assuming

- Per unit voltage magnitudes: $|v_i| = 1$ pu
- Negligible line resistances: $g_{ij} << b_{ij} \rightarrow g_{ij} = 0$
- Small voltage angle differences: $\sin(\theta_i - \theta_j) \approx \theta_i - \theta_j$

(2.3) then reduces to

$$\begin{aligned} f_{ij} &= b_{ij}(\theta_i - \theta_j) \\ \sum_{j:i\sim j} f_{ij} &= p^L, \end{aligned} \tag{2.4}$$

through which flows can be found for by solving a system of linear equations. It is clear upon inspection of (2.4) why this linearization is commonly referred to as DC load flow: if voltage angle and susceptance are replaced by voltage and conductance, one obtains Ohm's law for direct current networks. Until recently, power transmission was primarily AC, and the nickname for linearized power flow caused little confusion; however, given the increased usage of direct current transmission both at the high voltage transmission [11] and low voltage distribution [12] levels, a shift towards 'linearized' terminology may be appropriate.

In this work, we also use rectangular coordinates, in which case (2.1) is given by

$$\begin{aligned} p_{ij} &= g_{ij}(w_i^2 + x_i^2) + b_{ij}(w_i x_j - w_j x_i) - g_{ij}(x_i x_j + w_i w_j) \\ q_{ij} &= -b_{ij}(w_i^2 + x_i^2) + g_{ij}(w_i x_j - w_j x_i) + b_{ij}(x_i x_j + w_i w_j) \\ \sum_{j:i\sim j} p_{ij} &= p_i^L \\ \sum_{j:i\sim j} q_{ij} &= q_i^L \end{aligned} \tag{2.5}$$

The advantage of using (2.5) over (2.3) is that only quadratic polynomial nonlinearities appear, enabling concise application of the polynomial relaxations and conic optimizations discussed in the next two sections.

2.2 Conic optimization

Within convex optimization are special classes of problems which can be solved in polynomial time [6, 7, 78], which is to say that the computational effort it takes to solve a problem instance to within a prescribed error tolerance is in the worst case proportional to a polynomial in the number of variables and constraints. We note that no such guarantees exist for any metaheuristic, such as those mentioned in

the Introduction. Problems within these classes are expressible by linear equality constraints plus a particular cone constraint; the most well known and straightforward is the standard form linear program:

$$\min_z c^T z \quad \text{s.t.} \quad Az = b,\ z \geq 0.$$

The constraint $z \geq 0$ corresponds to the linear cone, or the positive orthant. Second-order cone [93] and semidefinite [118] programming are successive generalizations, which, although slower, are also solvable in polynomial time. Second-order cone and semidefinite constraints respectively have the form

$$\|Az + b\| \leq c^T z + d \quad \text{and} \quad X \succeq 0,$$

where $\succeq$ denotes positive semidefiniteness (i.e. $y^T X y \geq 0$ for all vectors y), and $\|\cdot\|$ the two-norm. We mention that, in practice, linear programming is often solved with the simplex algorithm, which has exponential worst case performance, but sometimes outperforms interior point methods, and leads to elegant mixed-integer constructions.

The application of conic optimization is nearly as broad as that of optimization itself; since the introduction of the simplex algorithm [37], linear programming has found usage across engineering and science. Second-order cone and semidefinite programming have more recently been used in developing both new formulations and relaxations in a number of fields, for example structural optimization [17], stochastic programming [93], robust optimization [16], and systems and control [100].

2.3 Lift-and-project relaxations

A relaxation of an optimization problem is any other optimization problem with a lower objective; of course, such a general definition is useless. Given an optimization problem based on certain data, we are more precisely interested in constructing easier optimization problems which take the same data as input, and produce tight lower bounds. The tools of choice in this thesis fall under what are known as lift-and-project

methods. In words, lift-and-project methods trade problems in difficult settings for larger problems in easier settings.

An initial application of lift-and-project methods was binary variables, which can be constrained polynomially with the equality $z^2 = z$ [94, 112]. The approach then gained substantial attention for the 0.878 semidefinite programming max-cut relaxation of [60]. In Chapter 3, we use spectral graph theory and semidefinite programming to relax a new class of multicommodity cut problems in similar fashion. Lift-and-project relaxations, particularly semidefinite versions, have since seen broad application via extremely general polynomial programming formulations [85,101,111]. In Chapter 4 we employ this perspective towards transforming nonconvex polynomial constraints into linear and then second-order cone and semidefinite constraints.

Before proceeding, we demonstrate the lift-and-project variant of [111] on two examples. First, consider the following bilinear optimization problem:

$$\begin{aligned} \min_{z} \quad & z_1 (z_2 - 1) \\ \text{s.t.} \quad & z_1 \geq 1, \quad z_2 \geq 2 \end{aligned}$$

A relaxation is formulated as follows. Add the redundant constraint $(z_1 - 1)(z_2 - 2) \geq 0$, and substitute a new variable y for all instances of $z_1 z_2$. The relaxation is given by

$$\begin{aligned} \min_{z,y} \quad & y - z_1 \\ \text{s.t.} \quad & z_1 \geq 1, \quad z_2 \geq 2, \quad y - 2z_1 - z_2 + 2 \geq 0 \end{aligned}$$

In this manner we lift polynomial problems with nonlinear constraints and objectives into higher dimensional spaces. Approximate solutions are obtained by then projecting the optimal relaxed solution onto the original space, which for our purposes means simply eliminating the new variables from the relaxed solution. Here, the minima of the original and relaxed problems are both one, with $z_1 = 1$, $z_2 = 2$, and $y = 2$. We say that a relaxed solution is tight if it coincides exactly with that of the original problem. Tightness is certified by the factorability of new variables into the original

ones; in this example, $y = z_1 z_2$. Although here the relaxed and actual minima are identical, it is not true in general, and usually will not be the case for transmission system planning problems.

Substitutions of any order can be performed within this framework, and it has been shown that as larger and larger constraint products are formed, the relaxation converges to the true optimum [87]. However, the sizes of the resulting linear programs grows rapidly, and so a compromise must be made at some point between accuracy and practicality.

As a second example, consider the optimal power flow relaxation of [89], which we make use of in Section 4.3.2. Take the rectangular coordinate formulation of power flow given in (2.5), and include it as constraints in an optimization problem with objective

$$\sum_i f_i\left(p_i^L\right). \tag{2.6}$$

Typical objectives include quadratic functions representing generator fuel costs [124], or real power loss, which is equal to the total generator power outputs minus the total demand. Create a vector $X = [w_1, x_1, \ldots, w_n, x_n]^T$, and set the $2n$ by $2n$ matrix $W = XX^T$. Then the following optimization problem is equivalent to (2.6) with (2.5) as constraints:

$$\min_{W,p,q,p^L,q^L} \quad \sum_i f_i\left(p_i^L\right) \tag{2.7}$$

$$\text{s.t.} \quad p_{ij} = g_{ij}(W_{i,i} + W_{i+n,i+n}) + b_{ij}(W_{i,j+n} - W_{j,i+n}) - g_{ij}(W_{i,j} + W_{i+n,j+n}) \tag{2.8}$$

$$q_{ij} = -b_{ij}^s(W_{i,i} + W_{i+n,i+n}) + g_{ij}(W_{i,j+n} - W_{j,i+n}) + b_{ij}(W_{i,j} + W_{i+n,j+n}) \tag{2.9}$$

$$\sum_{j:i\sim j} p_{ij} = p_i^L \tag{2.10}$$

$$\sum_{j:i\sim j} q_{ij} = q_i^L \tag{2.11}$$

$$W = XX^T \tag{2.12}$$

In the above optimization, the only source of nonconvexity is $W = XX^T$. A semidefinite relaxation in the spirit of [60] is obtained by replacing $W = XX^T$ with the equivalent pair $W \succeq 0$ and $\text{rank}(W) = 1$, and then dropping the latter constraint; we can interpret this as lifting the $2n$ voltage variables to the $2n(n+1)$ distinct variables in W. In [89], the relaxation is shown computationally to be exact on a large number of realistic instances, and dual conditions are given for assessing whether a given solution is tight.

2.4 Literature review

In each of the following three chapters, some subset of the prior contents of this section will be applied to a problem in or pertaining to power systems. We now provide a basic discussion of and literature review for each topic.

2.4.1 Spectral graph theory and multicommodity flow networks

Spectral graph theory, much of which concerns inequalities between eigenvalues of the graph Laplacian and NP-hard combinatorial optimization problems [33], traces its roots to a result in Riemannian geometry [28] and the identification of a connection between the smallest non-zero Laplacian eigenvalue and graph connectivity [53]. A lower and upper bound on a related eigenvalue quantifying bottlenecking in Markov chains was established in [42]. At present spectral graph theory sees broad application, including other theoretical contexts like expander graphs [10] and NP-hard graph cuts [97], divide and conquer algorithms [114], VLSI layout [84], and graph clustering and partitioning [99, 115].

Network flow is a nearby but for the most part disjoint field concerning a simple model of how quantities or commodities can travel through a capacitated graph or network [76]. A central result is the Max-Flow Min-Cut theorem [50, 75], which established the equivalence between the maximal flow that can be sent through a

graph and the smallest capacity cut separating source from destination, and explains the computational tractability of many single commodity network flow problems [4]. Applications of network flow are vast; broad examples include communications, transportation systems, and shipping routes, to name a few. There has been substantial theoretical interest in NP-hard graph cuts arising from the multicommodity case [72], namely the sparsest cut [114, 119]. Initial work began with linear programming approximations [90], and subsequent approaches have utilized the more general semidefinite programming along with randomized rounding procedures based on the max-cut relaxation of [60].

2.4.2 Transmission system planning

Transmission system planning is the straightforward problem of where to construct new transmission lines. For terrestrial systems, the problem is nearly always transmission system expansion planning, with the purpose of reinforcing an existing network to accommodate new load and generation. An additional note is that we specifically consider static, short-term transmission system expansion planning; the dynamic and long-term variants are both built upon the simpler version considered here.

As mentioned in the Introduction, an early optimization based approach led to the development of the first minimum spanning tree algorithm by Boruvka [23, 24]. The first mathematical programming formulation appeared in [57], which set a standard followed by nearly all subsequent approaches; a survey may be found in [88].

The equations of AC power flow combined with additional nonconvexity introduced by line construction variables necessitated the use of DC formulations, which up until recently in [106] accounted for all of the literature in the field. Approaches to the DC formulation may be divided into two sets: metaheuristics [105], e.g. genetic algorithms and particle swarms, and linear programming approximations [5, 107], notably the transportation, hybrid, and disjunctive models [21, 66, 68, 110, 121].

More recently, models have been expanded to contain additional factors, such as uncertainty [31] and economics [49].

2.4.3 Distribution system reconfiguration

Transmission systems carry power at high voltages over often long distances. Distribution systems, which are fed from transmissions systems by subtransmission lines, provide load to end users at lower voltages. Distribution systems often have loops, but are operated in a radial or tree configurations with certain switches open to enable detection and isolation of faults and failures [20]. A network may have numerous radial configurations attainable by different combinations of open and closed switches, and, in the absence of reliability objectives, switches may be used to alternate configurations based on secondary objectives, e.g. minimizing resistive losses [36]. These objectives, under the label quality of service, are also of significant interest to the all-electric ship [43]. In [13], the problem was considered further, and new objectives as well as a new power flow formulation specific to radial networks were introduced. Substantial analysis of the so-called *DistFlow* equations ensued [29, 30]; however, nearly all optimization approaches which followed made little use of their structure, using heuristics and metaheuristics to address the problem in black box fashion [40], as well as multiobjective approaches [39]. Relatively recently, a mixed-integer nonlinear programming approach was taken [81]. Separate from the terrestrial literature, a direct current mixed-integer linear programming formulation was used to reconfigure a shipboard power system for the purpose of restoring service to loads in the event of damage [26].

2.5 General perspective

In this chapter, conic programming has been identified as a relatively easy framework to solve optimization problems within, and lift-and-project methods as a general tool for transferring intractable optimization problems to conic programming; the bulk of this thesis focuses on applying this scheme to classical problems in power systems.

Fig. 2-1 depicts the relationships between each subject of this thesis. Conic optimization is the unifying tool, and is used to optimize transmission planning, reconfiguration, and ultimately approximate a new kind of multicommodity flow network

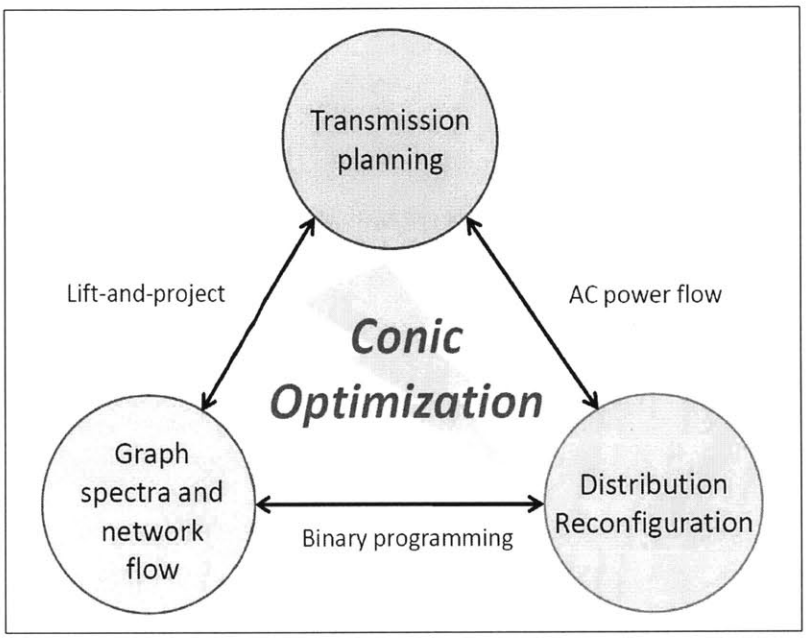

Figure 2-1: Relationships between chapters

cut.

An additional complication enters through integer variables. At present, linear and quadratic programming are the only mathematical programming frameworks with robust and efficient mixed-integer counterparts; however, as will be seen in this thesis, many mathematical descriptions of power systems are well approximated second-order cone and semidefinite expressions, yet contain large numbers of discrete variables. Mixed-integer second-order cone programming is an active area of research for which there is the expectation of eventually achieving the sophistication of the linear analogue [46, 120], and it is similarly within reason to expect subsequent development in the semidefinite case. In our discussions, we present mixed-integer linear and quadratic formulations as practical options, but also introduce mixed-integer second-order cone and semidefinite models in anticipation of future capabilities.

Chapter 3

Spectral graph theory and multicommodity flow networks

3.1 Introduction

Spectral graph theory [33] offers powerful tools for analysis and design of systems which are well modeled by graphs. However, many systems have important features not captured by purely graphical descriptions. Flow networks [4, 76] describe a wide variety of such systems, for example electric power grids and communication networks, yet have a minimal level detail additional to the underlying graph. In this work, we apply spectral graph theory to flow networks. We formulate a class of Laplacian matrix pencils for undirected, multicommodity flow networks and a Cheeger-like parameter which generalizes the sparsest cut [90, 114, 119], and relate them with bounds similar to the Cheeger inequality [28, 33, 42, 53]. When there are many commodities, finding the correct eigenvalue entails solving a combinatorial optimization problem, for which we formulate a semidefinite relaxation using the methodologies of [111] and [85]. In addition to flow networks, the multicommodity case may have application to many computer science problems modeled by cuts generalized by our development, such as graph partitioning [90], divide-and-conquer algorithms [114], and VLSI layout [84].

3.2 Background

3.2.1 The Laplacian of a graph and the Cheeger constant

We are given an undirected, connected graph G with vertices $V(G)$, edges $E(G)$, and corresponding adjacency matrix A. The Laplacian of G is defined as $L = D - A$ where D is a diagonal matrix with $D_{vv} = d_v = \sum_u A_{uv}$. The normalized Laplacian is $\mathcal{L} = D^{-1/2}LD^{-1/2}$, and its eigenvalues can be written $0 = \lambda_0 < \lambda_1 \leq \cdots \leq \lambda_{n-1} \leq 2$. The eigenvalues of $\mathcal{L}$ are equivalent to those of the generalized eigensystem $Lx - \lambda Dx = 0$, which is referred to as the pencil (L, D); for convenience we use this notation [61].

A fundamental construct from which many eigenvalue results originate is known as the Rayleigh quotient [71], which we now examine. Suppose J and K are symmetric matrices, let y be a vector, and consider the equation $Jy - \delta Ky = 0$. Multiplying by y^T, we have $y^TJy - \delta y^TKy = 0$, and hence $\delta = \frac{y^TJy}{y^TKy}$; this ratio is known as the Rayleigh quotient. To facilitate intuition about the mechanics employed later, we now give a basic theorem about the Rayleigh quotient:

Theorem 1 (Rayleigh-Ritz). *Let $\delta_{\min}$ be the minimum eigenvalue of the pencil (J, K), where J and K are positive semidefinite. Then*

$$\delta_{\min} = \min_y \frac{y^TJy}{y^TKy}.$$

Proof. Let $\delta_1, ..., \delta_n$ and $y_1, ..., y_n$ be the ascending-ordered eigenvalues and corresponding eigenvectors of (J, K). We first observe that we can equivalently minimize over vectors y for which $y^TKy = 1$, since clearly no vector of zero length about K will be a minimizer if J and K are positive semidefinite. Since J and K are symmetric positive semidefinite, $y_1, ..., y_n$ can be chosen orthonormal about K, and

$y = \xi_1 y_1 + \cdots + \xi_n y_n$ for some ξ with $\|\xi\| = 1$. We can then write

$$\begin{aligned}
\min_y \frac{y^T J y}{y^T K y} &= \min_{y: y^T K y = 1} y^T J y \\
&= \min_{\xi: \|\xi\| = 1} \left(\xi_1 y_1 + \cdots + \xi_n y_n\right)^T J \left(\xi_1 y_1 + \cdots + \xi_n y_n\right) \\
&= \min_{\xi: \|\xi\| = 1} \left(\xi_1 y_1 + \cdots + \xi_n y_n\right)^T K \left(\xi_1 \delta_1 y_1 + \cdots + \xi_n \delta_n y_n\right) \\
&= \min_{\xi: \|\xi\| = 1} \left(\xi_1^2 \delta_1 + \cdots + \xi_n^2 \delta_n\right)
\end{aligned}$$

The minimum is clearly attained for $\xi_1 = 1$ and $\xi_2 = \cdots = \xi_n = 0$, which completes the proof. One can use a nearly identical argument to show that

$$\delta_{\max} = \max_y \frac{y^T J y}{y^T K y}.$$

□

In Section 3.4.1, we will need to take special care when the second matrix in the pencil is indefinite. The Courant-Fischer theorem [71] is a generalization of the Rayleigh-Ritz theorem, which characterizes all of the eigenvalues in the spectrum in terms of subspaces spanned by the eigenvectors. We will make immediate use of the following characterization of the second smallest eigenvalue:

$$\delta_2 = \min_{y \perp y_1} \frac{y^T J y}{y^T K y}.$$

We now return to the pencil (L, D). Let f be a function assigning a complex value $f(v)$ to each vertex v, where the notation f denotes the vector of these values. The Rayleigh quotient of (L, D) is

$$\frac{\sum_{u \sim v} (f(u) - f(v))^2}{\sum_v f(v)^2 d_v},$$

where the sum subscript $u \sim v$ denotes summation over all pairs of vertices connected by edges. The first nonzero eigenvalue, often called the algebraic connectivity [53],

satisfies

$$\lambda_1 = \inf_{f \perp D\mathbf{1}} \frac{\sum_{u \sim v} (f(u) - f(v))^2}{\sum_v f(v)^2 d_v}.$$

The Cheeger constant [28, 33, 42, 53], sometimes referred to as the conductance, is a measure of the level of bottlenecking in a graph, as illustrated in the left plot of Fig. 3-1. It is defined

$$h = \min_X \frac{\left|C\left(X, \bar{X}\right)\right|}{\min\left(\text{vol}(X), \text{vol}\left(\bar{X}\right)\right)},$$

where $C(X, \bar{X})$ is the set of edges with only one vertex in X, $\left|C(X, \bar{X})\right| = \sum_{u \in X, v \in \bar{X}} A_{uv}$, and $\text{vol}(X) = \sum_{v \in X} d_v$. h is related to the algebraic connectivity by what is known as the Cheeger inequality:

$$2h \geq \lambda_1 > \frac{h^2}{2}.$$

3.2.2 Flow networks

A flow network is a weighted graph on which flows travel between vertices by way of the edges [4, 76]. In this work we only consider undirected flow networks. Suppose further that we have a multicommodity flow network with m different types of flows or commodities [72], and that we are given a supply and demand vector for each commodity i, p^i, which satisfies $\sum_v p_v^i = 0$.

We denote the flow of commodity i from u to v by $g_i(u, v)$, and the weight of the edge between u and v by $c(u, v)$, which we refer to as a capacity. In this work, we equate capacities with edge weights such that the capacity of an edge, $c(u, v)$, is identical to its weight in the graph adjacency matrix, A_{uv}. We say that a flow network is feasible if there exists a flow $g_i : V(G) \times V(G) \to \mathbb{R}^+$ satisfying $\sum_{i=1}^m g_i(u, v) \leq c(u, v)$, and $\sum_v g_i(u, v) - g_i(v, u) = p_u^i$.

Network flow straightforwardly model a large number of real systems, and quantities p_v^i and $c(u, v)$ deserve some concrete interpretation; as the remainder of this thesis is specific to electric power systems, which are crudely approximated by single-commodity flow networks, they are an appropriate context. The vector of supply and demand p is analogous to a vector of bus load (demand) and generation (supply). The capacity of an edge $c(u, v)$ in this case represents a transmission line thermal

limit, restricting the flow of real or apparent power. The structure of the Laplacian matrix of capacities, L, however, has identical structure to the standard bus admittance matrix [124]; here it is essentially the same matrix, but with capacities rather than admittances.

For many purposes, a network with multiple sources and sinks can be reduced to one with a single source and sink by introducing a super-source and super-sink [76], for example maximizing the flow through a network. As will be seen in the next section, this simplification is not compatible with our development, and so we allow as many vertices as are in the network to be sources or sinks provided that the total flow is conserved.

3.3 A flow-based Cheeger constant

We identify a quantity which measures bottlenecking of flows rather than graphical structure, a shown in the right plot of Fig. 3-1, and is in fact a generalization of the sparsest cut [90]. We begin with the single commodity version. Define

$$q = \min_X \frac{\left|C\left(X, \bar{X}\right)\right|}{\left|\sum_{v \in X} p_v\right|}.$$

The denominator is the flow that would be sent from X to $\bar{X}$ in the absence of edge capacities. By the max-flow min-cut theorem, the actual flow from X to $\bar{X}$ can be no greater than $\left|C\left(X, \bar{X}\right)\right|$ [50, 75]. In fact, it is well known that $q \geq 1$ is also a sufficient condition for the existence of a feasible flow [56, 70]; an implication is that q is not NP-hard when there is only one commodity.

Before discussing the multicommodity case, we give a brief example for which the introduction of a super-source changes the value of q. Consider a three vertex line graph with $p = [1, -2, 1]^T$ and $c(1,2) = 3$ and $c(2,3) = 2$. Simple calculation gives $q = 2$ and $C(X, \bar{X}) = c(2,3)$ for this network. Now append a super-source with $p_s = 2$, connected to vertices one and three by edges of unit capacity, and set p_1 and p_3 to zero. The optimal q for the modified network is $q = 1$, and furthermore the

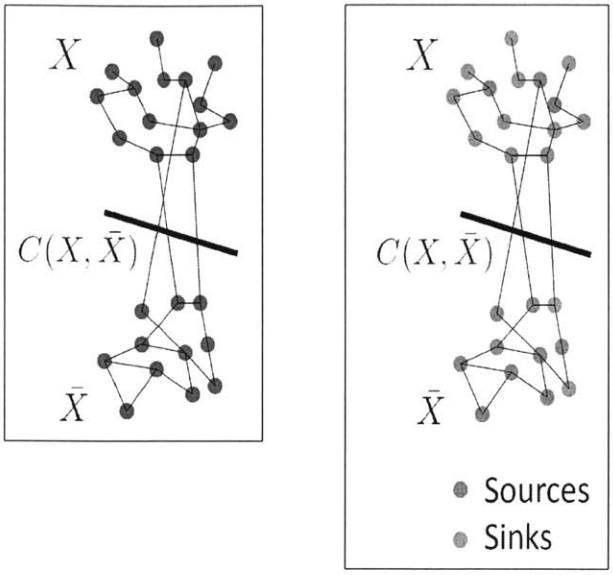

Figure 3-1: Graph bottlenecking as measured by h (left) versus flow bottlenecking as measured by q (right)

optimal cut has changed so that vertices one and three are now on the same side. Hence the usual simplification of multi-source, multi-sink problems to single-source, single-sink problems is not applicable here.

We now generalize q to multicommodity flow networks. Let $\kappa \in \{-1, 1\}^m$ and $p_v^\kappa = \sum_{i=1}^m \kappa^i p_v^i$, where κ^i is element i of κ, and define

$$S(X) = \max_\kappa \sum_{v \in X} p_v^\kappa.$$

Because the objective is linear in κ, it is equivalent to the continuous linear optimization problem in which $\kappa \in [-1, 1]^m$. The purpose of the maximization is merely to ensure that the net-demand which would leave set X of each commodity has the same sign. We then define the multicommodity version to be

$$q = \min_X \frac{\left|C\left(X, \bar{X}\right)\right|}{S(X)}, \tag{3.1}$$

which in matrix form is given by

$$q = \min_{x \in \{0,1\}^n, \kappa} \frac{x^T L x}{|x^T P_\kappa x|}, \tag{3.2}$$

where P_κ is a matrix with p^κ on the main diagonal and zeros elsewhere.

q also has the minimax network flow formulation

$$\begin{aligned} q = \min_{\kappa} \max_{g,\tau} \quad & \tau \\ \sum_{u:u\sim v} g_{uv} - g_{vu} &= \tau p_v^\kappa \quad \forall v \\ 0 \le g_{uv} &\le A_{uv} \quad \forall u \sim v \\ -1 \le \kappa^i &\le 1 \quad \forall i \end{aligned} \tag{3.3}$$

Intuitively, we are optimally consolidating the supplies and demands into a single commodity, the maximum flow of which is equal to the minimum cut by the max-flow min-cut theorem and the result of [56, 70].

3.4 Laplacians for flow networks

We now derive Cheeger-like inequalities for eigenvalues of flow normalized Laplacians. Note that we have not assumed feasibility, rather only that $\sum_v p_v^i = 0$ for each commodity i. The pencil (L, P_κ) is a natural starting point because its smallest magnitude eigenvalue is a continuous relaxation of q. However, it is defective, which is to say that an eigenfunction is missing. It has two zero eigenvalues corresponding to the constant eigenfunction; in the simplest case of a two vertex network, the eigenvalues provide no meaningful information.

3.4.1 Variational formulation

We can see why (L, P_κ) is defective by considering the quotient

$$\frac{f^T P_\kappa f}{f^T L f}.$$

It is undefined at $f = \mathbf{1}$, but approaches infinity as f approaches $\mathbf{1}$ from any direction. Now consider the perturbed pencil $\left(P_\kappa, L + a\mathbf{1}\mathbf{1}^T\right)$ for $a > 0$, the eigenvalues of which are one over those of $\left(L + a\mathbf{1}\mathbf{1}^T, P_\kappa\right)$: it is similar to $\sqrt{L + a\mathbf{1}\mathbf{1}^T} P_\kappa \sqrt{L + a\mathbf{1}\mathbf{1}^T}$, which can be real symmetric because $L + a\mathbf{1}\mathbf{1}^T$ is positive definite. By the Rayleigh-Ritz theorem [71], the largest positive and negative eigenvalues satisfy

$$\sup_f \frac{f^T P_\kappa f}{f^T \left(L + a\mathbf{1}\mathbf{1}^T\right) f} \quad \text{and} \quad \inf_f \frac{f^T P_\kappa f}{f^T \left(L + a\mathbf{1}\mathbf{1}^T\right) f}.$$

As a approaches zero, the two eigenvalues will approach positive and negative infinity. This is distinctly a consequence of $\mathbf{1}$ being in the null space of L and the fact that $\mathbf{1}^T P_\kappa \mathbf{1} = 0$; were the latter not true, only one of the eigenvectors could converge to $\mathbf{1}$ and not cause the quotient to switch signs.

The zero eigenvalue of (L, P) does have a generalized eigenfunction, as guaranteed by the Jordan canonical form theorem [71]. Solving the equation $(L - 0P_\kappa)\, x = P_\kappa \mathbf{1}$ yields $x = L^\dagger p^\kappa$, where $L^\dagger$ is the Moore-Penrose pseudo-inverse of L.

We rectify (L, P_κ) by adding an infinite rank-one perturbation. Consider either of the pencils $\lim_{b\to\infty} \left(L + brr^T, P_\kappa\right)$ and $\lim_{b\to\infty} \left(L, P_\kappa + brr^T\right)$, where $r \in \mathbb{R}^n$ is not orthogonal to $\mathbf{1}$. They will respectively have an infinite and a zero eigenvalue, both corresponding to the eigenfunction r, and will share the remaining eigenvalues and eigenfunctions.

Because both matrices of the pencil are real symmetric and the left matrix is positive definite, the eigenvalues and eigenfunctions are real and admit a variational characterization. The magnitude of the smallest, which we denote μ_κ^r, has the varia-

tional characterization

$$\begin{aligned}\mu_\kappa^r &= \lim_{b\to\infty} \inf_f \left| \frac{f^T \left(L + brr^T\right) f}{f^T P_\kappa f} \right| \\ &= \inf_{f \perp r} \left| \frac{f^T L f}{f^T P_\kappa f} \right|. \end{aligned} \tag{3.4}$$

Define

$$\mu^r = \min_\kappa \mu_\kappa^r. \tag{3.5}$$

Even for the simple case in which r is not a function of κ, a continuous relaxation of (3.5) is not guaranteed to have a unique global minimum. This is evident from the reciprocal

$$(\mu^r)^{-1} = \max_\kappa \sup_{f \perp r} \left| \frac{f^T P_\kappa f}{f^T L f} \right|,$$

which is the maximum of the pointwise supremum of a family of linear functions of κ, and hence a convex maximization problem [25]. A consequence is that there is no easy way of computing μ^r when there are many commodities; however, when the number of commodities is small, it may be straightforward to guess the optimal κ, or simply try all of the likely ones. Furthermore, convexity does guarantee that the optimal κ is at a corner, and thus the continuous relaxation is equivalent to the binary formulation.

3.4.2 Bounds on μ^r

We have the following Cheeger-like inequality:

Theorem 2.

$$\frac{q \left|\sum_v r_v\right|}{\left|\sum_{v\in X} r_v - \sum_{v\in \bar{X}} r_v\right|} \geq \mu^r > \frac{qh \left|\sum_v r_v\right|}{2\sqrt{\sum_v d_v \sum_v \left|r_v^2\right| / d_v}},$$

where X is the vertex set associated with q and $r \in \mathbb{R}^n$.

Proof. The structure of our proof for the most part follows that of the Cheeger inequality given in [33]. Although we assume unit capacities, the proof straightforwardly

extends to networks with non-negative capacities by generalizing the definition of the Laplacian to allow for weighted graphs.

We begin with the upper bound. Define the function

$$f(v) = \begin{cases} \sum_{u \in X} r_u & \text{if } v \in \bar{X} \\ -\sum_{u \in \bar{X}} r_u & \text{if } v \in X \end{cases},$$

where X is the optimal vertex set associated with q. Let κ_1 and κ_2 be optimal for (3.1) and (3.5), respectively. Substituting f into (3.4) gives

$$\begin{aligned} \mu^r &\leq \mu^r_{\kappa_1} \\ &\leq \frac{\left|C\left(X, \bar{X}\right)\right| \left|\left(\sum_{v \in X} r_v + \sum_{v \in \bar{X}} r_v\right)^2\right|}{S(X) \left|\left(\sum_{v \in X} r_v\right)^2 - \left(\sum_{v \in \bar{X}} r_v\right)^2\right|} \\ &= \frac{q \left|\sum_v r_v\right|}{\left|\sum_{v \in X} r_v - \sum_{v \in \bar{X}} r_v\right|}. \end{aligned}$$

We now prove the lower bound. Let f be the eigenfunction of $\lim_{b \to \infty}(L + brr^T, P_{\kappa_2})$ associated with $\mu^r_{\kappa_2}$. Order the vertices in $V(G)$ so that $|f(v_i)| \leq |f(v_{i+1})|$ for $i = 1, ..., n-1$. For each i define the cut $D_i = \{\{j, k\} \in E(G) \mid 1 \leq j \leq i < k \leq n\}$, and set

$$\alpha = \min_{1 \leq i < n} \frac{|D_i|}{\left|\sum_{j \leq i} p_j^{\kappa_2}\right|}.$$

By definition, $\alpha \geq q$ regardless of whether or not $\kappa_1 = \kappa_2$. We have

$$\begin{aligned} \mu^r &= \left| \frac{\sum_{u \sim v} (f(v) - f(u))^2 \sum_{u \sim v} (f(v) + f(u))^2}{\sum_v f(v)^2 p_v^{\kappa_2} \sum_{u \sim v} (f(u) + f(v))^2} \right| \\ &\geq \left| \frac{\left(\sum_{u \sim v} |f(u)^2 - f(v)^2|\right)^2}{2 \sum_v f(v)^2 p_v^{\kappa_2} \sum_v f(v)^2 d_v} \right| \quad \text{by Cauchy-Schwartz} \\ &= \left| \frac{\left(\sum_i |f(v_i)^2 - f(v_{i+1})^2| \, |D_i|\right)^2}{2 \sum_v f(v)^2 p_v^{\kappa_2} \sum_v f(v)^2 d_v} \right| \quad \text{by counting} \end{aligned}$$

$$
\begin{aligned}
&\geq \left| \frac{\left(\sum_i \left(f(v_i)^2 - f(v_{i+1})^2\right) \alpha \left|\sum_{j\leq i} p_{v_j}^{\kappa_2}\right|\right)^2}{2\sum_v f(v)^2 p_v^{\kappa_2} \sum_v f(v)^2 d_v} \right| && \text{by the definition of } \alpha \\
&\geq \left| \frac{\alpha^2 \left(\sum_i \left(f(v_i)^2 - f(v_{i+1})^2\right) \sum_{j\leq i} p_{v_j}^{\kappa_2}\right)^2}{2\sum_v f(v)^2 p_v^{\kappa_2} \sum_v f(v)^2 d_v} \right| && \text{by the triangle inequality} \\
&\geq \left| \frac{q^2 \left(\sum_i f(v_i)^2 \left(\sum_{j\leq i} p_{v_j}^{\kappa_2} - \sum_{j\leq i-1} p_{v_j}^{\kappa_2}\right)\right)^2}{2\sum_v f(v)^2 p_v^{\kappa_2} \sum_v f(v)^2 d_v} \right| \\
&= \left| \frac{q^2 \left(\sum_i f(v_i)^2 p_{v_i}^{\kappa_2}\right)^2}{2\sum_v f(v)^2 p_v^{\kappa_2} \sum_v f(v)^2 d_v} \right| \\
&= \left| \frac{q^2 \sum_v f(v)^2 p_v^{\kappa_2}}{2\sum_v f(v)^2 d_v} \right|.
\end{aligned}
$$

Switching to matrix notation and noting that $\mu^r f^T P_{\kappa_2} f = -f^T L f$, we simplify further so that

$$
\mu^r \geq \frac{q^2 f^T L f}{2\mu^r f^T D f}.
$$

Multiplying through by μ^r and taking the positive square root, we have that

$$
\begin{aligned}
\mu^r &\geq q\sqrt{\frac{f^T L f}{2 f^T D f}} \\
&\geq q\sqrt{\frac{\lambda_r}{2}},
\end{aligned}
$$

where λ_r is the smallest eigenvalue of the pencil $\lim_{b\to\infty}(L + brr^T, D)$.

λ_r may not be an intuitive quantity in some cases, so we also derive a slightly looser but more revealing lower bound, which is a function of λ_1 and thus h, by the Cheeger inequality. Using similarity and the substitution $l = D^{1/2} f$, we have

$$
\mu^r \geq q\sqrt{\frac{l^T \mathcal{L} l}{2 l^T l}}.
$$

Because $D^{1/2}\mathbf{1}$ is in the null space of $\mathcal{L}$, l in the numerator can be replaced with its

projection onto the orthogonal complement of $D^{1/2}\mathbf{1}$, which we denote $\text{proj}_{D^{1/2}\mathbf{1}^\perp}(l)$. The minimum possible ratio of their lengths is given by

$$\beta = \min_{c \perp D^{-1/2}r} \frac{\|\text{proj}_{D^{1/2}\mathbf{1}^\perp}(c)\|}{\|c\|} = \min_{c \perp D^{-1/2}r} \frac{\|c - \text{proj}_{D^{1/2}\mathbf{1}}(c)\|}{\|c\|}. \tag{3.6}$$

The minimizing c is

$$\bar{c} = \text{proj}_{D^{-1/2}r^\perp}\left(D^{1/2}\mathbf{1}\right) = D^{1/2}\mathbf{1} - \text{proj}_{D^{-1/2}r}\left(D^{1/2}\mathbf{1}\right).$$

Substituting $\bar{c}$ into (3.6), after some algebra, yields

$$\beta = \frac{\left|\mathbf{1}^T r\right|}{\|D^{1/2}\mathbf{1}\| \, \|D^{-1/2}r\|} = \frac{\left|\sum_v r_v\right|}{\sqrt{\sum_v d_v \sum_v r_v^2/d_v}}.$$

Let k be a vector the same length as l and parallel to $\text{proj}_{D^{1/2}\mathbf{1}^\perp}(l)$. We then have

$$\begin{aligned} \mu^r &\geq q\beta\sqrt{\frac{k^T\mathcal{L}k}{2l^Tl}} \\ &\geq q\beta\sqrt{\frac{\lambda_1 \|k\|^2}{2\|l\|^2}} \\ &= q\beta\sqrt{\frac{\lambda_1}{2}} \\ &> \frac{qh\beta}{2}. \end{aligned}$$

□

3.4.3 Orthogonality constraints

It is important that the upper bound stays finite for all networks of interest; for some r, there are certain networks which will cause the denominator to be zero, constituting an effective blindspot in μ^r. For analysis of a single network, one might heuristically construct an r for which it is clear that this can not happen. Design and optimization however require that the upper bound remains finite for all possible networks, or else an algorithm may simply seek out networks for which the upper bound is infinite.

We now examine several choices of r.

1. The maximum possible lower bound is $qh/2$, which is attained by $r = D\mathbf{1}$. Unfortunately, the upper bound then becomes

$$\mu^{D\mathbf{1}} \leq \frac{q\text{vol}\left(V(G)\right)}{\left|\text{vol}(X) - \text{vol}\left(\bar{X}\right)\right|},$$

which is infinite if the sums of the degrees on either side of $C\left(X, \bar{X}\right)$ are equal. This is reflected in $\mu^{D\mathbf{1}}$ as well: consider a symmetric 'dumbbell' network in which two identical halves are connected by a single edge, and assume that all vertices in one half are unit sources and in the other half unit sinks of a single commodity. As the size of the halves is increased, it can be observed that $\mu^{D\mathbf{1}}$ grows despite q_1 decreasing as one over the number of vertices.

2. q has a number of interpretations in which being larger is better, so we are interested in choices for which it is the only non-constant factor in the upper bound. Let $Y \subseteq X$ or $Y \subseteq \bar{X}$. If we choose r to be

$$\delta_v^Y = \begin{cases} d_v & \text{if } v \in Y \\ 0 & \text{if } v \in \bar{Y} \end{cases}, \tag{3.7}$$

the bound becomes

$$q \geq \mu^{\delta^Y} > \frac{qh}{2}\sqrt{\frac{\text{vol}(Y)}{\text{vol}(V(G))}}.$$

This may somewhat impractical for most choices of Y, particularly in contexts in which the edges and hence X can change. However, if Y is the singleton z, X need not be known, and $\text{vol}(Y)$ is simply replaced by d_z. The formulation is simple in this case, but the dependence on the vertex z and the potential $1/\sqrt{n}$ factor in the lower bound may be undesirable.

3. Rather than using a single orthogonality constraint, taking the minimum of two eigenvalues can result in an upper bound which is always finite. For a vertex set N, let N^+ (N^-) denote the subset for which $p_v^{\kappa_1} > 0$ ($p_v^{\kappa_1} < 0$), $v \in N$, where

κ_1 is optimal for (3.1). Consider

$$s_v^+ = \begin{cases} p_v^\kappa & v \in V(G)^+ \\ 0 & v \in V(G)^- \end{cases} \text{ and } s_v^- = \begin{cases} p_v^\kappa & v \in V(G)^- \\ 0 & v \in V(G)^+ \end{cases}, \tag{3.8}$$

and set $\mu^s = \min\left\{\mu^{s^+}, \mu^{s^-}\right\}$. The upper bound of the minimum of the two resulting eigenvalues is

$$\mu^s \leq \min\left\{ \frac{q\sum_{v\in V(G)^+} p_v^{\kappa_1}}{\left|\sum_{v\in X^+} p_v^{\kappa_1} - \sum_{v\in \bar{X}^+} p_v^{\kappa_1}\right|}, \frac{-q\sum_{v\in V(G)^-} p_v^{\kappa_1}}{\left|\sum_{v\in X^-} p_v^{\kappa_1} - \sum_{v\in \bar{X}^-} p_v^{\kappa_1}\right|} \right\}.$$

Observe that

$$\begin{aligned} 2S(X) &= \left|\sum_{v\in X} p_v^{\kappa_1} - \sum_{v\in \bar{X}} p_v^{\kappa_1}\right| \\ &\leq \left|\sum_{v\in X^+} p_v^{\kappa_1} - \sum_{v\in \bar{X}^+} p_v^{\kappa_1}\right| + \left|\sum_{v\in X^-} p_v^{\kappa_1} - \sum_{v\in \bar{X}^-} p_v^{\kappa_1}\right|. \end{aligned}$$

Because the numerators are equal, we have

$$\mu^s \leq \frac{q\sum_v |p_v^{\kappa_1}|}{2S(X)},$$

which is finite because $S(X)$ is always greater than zero. Under certain conditions, μ^s is bounded above by q, as shown in the computational example in Section 3.7.1 and by the following lemma.

Lemma 1. *Suppose $V(G)^+ \subseteq X$ or $V(G)^- \subseteq X$. Then $\mu^s \leq q$.*

Proof. Let P^+ (P^-) be a matrix with s^+ (s^-) on the main diagonal and zeros elsewhere, and let x be the minimizer of (3.2). We have

$$\begin{aligned} q &= \frac{x^T L x}{|x^T P_{\kappa_1} x|} \\ &= \frac{x^T L x}{|x^T P^+ x + x^T P^- x|} \end{aligned}$$

$$
\begin{aligned}
&\geq \min\left\{\frac{x^TLx}{x^TP^+x}, \frac{x^TLx}{|x^TP^-x|}\right\} \qquad \text{by the definiteness of } P^+ \text{ and } P^- \\
&\geq \min\left\{\min_{x\in\{0,1\},x\perp s^-}\frac{x^TLx}{x^TP^+x}, \min_{x\in\{0,1\},x\perp s^+}\frac{x^TLx}{|x^TP^-x|}\right\} \qquad \text{by the assumption} \\
&= \min\left\{\min_{x\in\{0,1\},x\perp s^-}\frac{x^TLx}{|x^TP_{\kappa_1}x|}, \min_{x\in\{0,1\},x\perp s^+}\frac{x^TLx}{|x^TP_{\kappa_1}x|}\right\} \\
&\geq \min\left\{\min_{\kappa,x\perp s^-}\frac{x^TLx}{|x^TP_{\kappa}x|}, \min_{\kappa,x\perp s^+}\frac{x^TLx}{|x^TP_{\kappa}x|}\right\} \\
&= \min\left\{\mu^{s^-}, \mu^{s^+}\right\}.
\end{aligned}
$$

□

4. Lastly we mention a complex orthogonality condition, for which the theory of the preceding section does not hold. Define

$$
t_v = \begin{cases} p_v^\kappa & \text{if } p_v^\kappa \geq 0 \\ ip_v^\kappa & \text{if } p_v^\kappa < 0 \end{cases}.
$$

Based on observation, we conjecture the following bound:

$$
\frac{q\sum_v |p_v^{\kappa_1}|}{2S(X)} \geq \mu^t \geq \mu^s.
$$

3.4.4 Calculation via orthogonal transformation

One method by which to numerically compute μ^r using standard eigenvalue solvers is to approximate the limit of the pencil with a large number in place of b. This can be unsatisfactory because if the number isn't large enough, the approximation is poor, while if it is too large numerical inaccuracies may arise, particularly for large networks. An orthogonal transformation can instead be used to obtain the exact answer.

Let R be an orthonormal matrix with first column equal to $r/\|r\|$. Because eigenvalues are invariant under orthogonal transformation, those of $\lim_{c\to\infty}(R^TLR + bR^Trr^TR, R^TP_\kappa R)$ are identical to those of $\lim_{c\to\infty}(L + brr^T, P_\kappa)$. Let L' and P' be

the respective bottom right $n-1$ by $n-1$ submatrices of $R^T L R$ and $R^T P_\kappa R$. The eigenfunction with the infinite eigenvalue is the last column of $R^T L R$, and hence the remaining eigenvalues (among which is μ^r) are given by the reduced pencil (L', P'), which can be solved by any generalized eigenvalue algorithm. We remark that when $r = \delta^z$, this amounts to simply removing row and column z from L and P_κ.

3.5 An alternate relaxation of q

We now examine a slightly different formulation of q and arrive a quantity similar to μ^r_κ, but which scales as capacity over flow squared. This has relevance in certain scenarios such as electrical current flow, which is conserved in networks, yet is proportional to the square root of power loss.

Consider the minimization

$$\min_{x \in \{0,1\}} \frac{x^T L x}{|x^T p^\kappa|}.$$

If $\kappa = \kappa_1$, the minimum is q. Relaxing x to take on continuous values and introducing the constraint $\left|x^T p^\kappa\right| = 1$ yields

$$\gamma_\kappa = \min_{|x^T p^\kappa|=1} \frac{x^T L x}{|x^T p^\kappa|} \tag{3.9}$$

$$= \frac{1}{p^{\kappa T} L^\dagger p^\kappa}. \tag{3.10}$$

We first make two observations: γ_κ is the sole finite eigenvalue of the pencil $\left(L, p^\kappa p^{\kappa T}\right)$, and the optimal x associated with γ_κ, $L^\dagger p^\kappa / \gamma_\kappa$, is proportional to the generalized eigenvector of the zero eigenvalue of (L, P_κ).

Let

$$\gamma = \min_\kappa \gamma_\kappa, \tag{3.11}$$

and let κ_3 be optimal. A continuous relaxation of κ is again of little value here: because $L^\dagger$ is positive semidefinite, it becomes a concave minimization problem, for which there will likely be multiple local minima.

We bound γ from above using q in the same fashion as μ^r.

Lemma 2.

$$\gamma \leq \frac{q}{S(X)}$$

Proof. Let

$$x(v) = \begin{cases} \frac{1}{S(X)} & \text{if } v \in X \\ 0 & \text{if } v \in \bar{X} \end{cases},$$

Substituting x into (3.9), we have

$$\begin{aligned} \gamma &\leq \gamma_{\kappa_1} \\ &\leq \frac{\left|C\left(X, \bar{X}\right)\right|}{S(X)^2} \\ &= \frac{q}{S(X)}. \end{aligned}$$

□

We can draw further comparison with current flow by considering resistive power loss in a direct current electrical network. Let p be the vector of currents entering and exiting the network through the vertices. Define the admittance Laplacian L_A to be the Laplacian with admittance (one over resistance) edge weights. The total power dissipated is

$$p^T L_A^\dagger p,$$

which is exactly $1/\gamma$ for the single commodity case.

3.6 Semidefinite programming with many commodities

When there are many commodities, the minimizations over κ in (3.5) and (3.11) can pose intractable combinatorial optimization problems. Since its application to the max-cut problem [60], semidefinite programming [25, 118] has seen wide usage in developing relaxations for NP-hard problems, the most pertinent example here being the sparsest cut problem [9, 10, 59]. We apply the methodology of [111] and [85] to

(3.5) and (3.11) and obtain simple semidefinite relaxations of μ^r and γ. As applied to the sparsest cut problem, these relaxations are less accurate than those based on geometric formulations [9, 10], but constitute a new approach in approximating the more general q.

3.6.1 Relaxing μ^r

As shown in the previous sections, the orthogonality condition can be chosen so that μ^r is a lower bound for q. We formulate a semidefinite programming relaxation of (3.5), which consequently is also a relaxation of q.

μ^r can be expressed in terms of semidefinite programming as the following minimax problem:

$$\begin{aligned} \min_{\kappa} \max_{\xi} \quad & \xi \\ \\ & \xi P_\kappa \preceq \lim_{b\to\infty} L + brr^T \\ & -1 \leq \kappa^i \leq 1 \quad \forall i \end{aligned} \tag{3.12}$$

As long as the graph is connected, h, q and therefore μ^r are greater than zero, and so (3.12) is strictly feasible. We can thus replace the inner maximization with its dual and obtain the equivalent bilinear semidefinite program

$$\begin{aligned} \min_{\kappa,Z} \quad & \mathbf{Tr}\ LZ \\ \\ & \mathbf{Tr}\ rr^T Z = 0 \\ & \mathbf{Tr}\ P_\kappa Z = 1 \\ & 0 \preceq Z \\ & -1 \leq \kappa^i \leq 1 \quad \forall i \end{aligned} \tag{3.13}$$

where **Tr** denotes the trace operator.

If the first constraint is dropped, we obtain the result of applying the original max-cut relaxation of [59] to (3.2); this modification is of course always zero, as it corresponds to the defective pencil (L, P_κ). The first constraint makes the relaxation

nontrivial, and can be designed according to Section 3.4.3.

The second constraint of (3.13) is bilinear and hence nonconvex. We proceed to formulate the simplest nontrivial relaxation within the framework of [85, 111]. Let P^i be a diagonal matrix with p^i, the vector of commodity i's supplies and demands, on its main diagonal. Note that $P_\kappa = \sum_{i=1}^m \kappa^i P^i$. Introduce a matrix W^i for each commodity i, and substitute W_i for each instance of the product $\kappa^i Z$. An additional constraint on each W_i is constructed by taking the product of the last two constraints. The resulting semidefinite relaxation is given by

$$\begin{aligned}
\min_{Z,W^i} \quad & \mathbf{Tr}\ LZ \\
& \\
& \mathbf{Tr}\ rr^T Z = 0 \\
& \mathbf{Tr}\ rr^T W^i = 0 \quad \forall i \\
& \mathbf{Tr} \sum_{i=1}^m P^i W^i = 1 \\
& 0 \preceq Z \\
& -Z \preceq W^i \preceq Z \quad \forall i
\end{aligned} \tag{3.14}$$

As stated, (3.14) is an unwieldy relaxation due to the large number of new variables introduced. When r is an indicator vector, we can reduce the size by recognizing that often most vertices are not sources or sinks of most commodities, for example in the sparsest cut problem, in which each commodity is attached to only two vertices.

Let $r = \delta^1$ (without loss of generality one can relabel the vertices so that any vertex, e.g. that of maximum degree, is the first). Define M^i to be the set of vertices v for which p^i_v is nonzero. Let $Z(M^i)$ denote the $|M^i|$ by $|M^i|$ principal submatrix of Z induced by the set M^i, and likewise let $P^i(M^i)$ denote the corresponding $|M^i|$ by $|M^i|$ submatrix of P^i. Note that the condition $Z \succeq 0$ implies that every principal submatrix of Z is positive semidefinite. Again substituting a matrix W^i wherever $\kappa^i Z(M^i)$ appears, we have the equivalent semidefinite program

$$\min_{Z,W^i} \quad \mathbf{Tr}\ LZ$$

$$\begin{aligned} & Z_{11} = 0 \\ & W^i_{11} = 0 \quad \forall i : 1 \in M^i \\ & \mathbf{Tr} \sum_{i=1}^{m} P^i\left(M^i\right) W^i = 1 \\ & 0 \preceq Z \\ & -Z\left(M^i\right) \preceq W^i \preceq Z\left(M^i\right) \quad \forall i \end{aligned} \tag{3.15}$$

If, given an optimal solution $\tilde{Z}$ and $\tilde{W}^i$ to (3.14) or (3.15), there exists $\tilde{\kappa}^i \in [-1, 1]$ such that $\tilde{Z} = \tilde{\kappa}^i \tilde{W}^i$ (respectively $\tilde{Z}\left(M^i\right) = \tilde{\kappa}_i \tilde{W}^i$) for each i, $\tilde{Z}$ and $\tilde{\kappa}^i$ are optimal for (3.13). In general, however, the relaxation is not tight, so we suggest the following rounding heuristic: if $\mathbf{Tr}\ \tilde{W}^i > 0$, set $\tilde{\kappa}^i = 1$, otherwise set $\tilde{\kappa}^i = -1$ for each i. Once $\tilde{\kappa}$ is known, the corresponding approximation to q is equal to the optimum of the linear program obtained by removing the outer minimization of (3.3) and setting $\kappa = \tilde{\kappa}$.

A natural question is whether linear relaxations can be directly formulated from (3.3). Repeating the steps used to obtain (3.14) from (3.12), one can apply the relaxation of [111] to the resulting bilinear program. We observed that a 'second order' linear relaxation was uniformly zero; while higher order relaxations are possible, they are cumbersome in size, and furthermore it has been shown that the corresponding semidefinite relaxations of [85] are more efficient and numerically superior [86].

3.6.2 Relaxing γ

The reciprocal of (3.11) can be written

$$\max_{\kappa \in \{-1,1\}^m} p^{\kappa T} L^\dagger p^\kappa = \max_{\kappa \in \{-1,1\}^m} \sum_{i=1}^{m} \sum_{j=1}^{m} \kappa^i \kappa^j p^{i T} L^\dagger p^j.$$

A simple semidefinite relaxation in the fashion of [59] is

$$\begin{aligned} \max_{K} \quad & \sum_{i=1}^{m}\sum_{j=1}^{m} K_{ij} p^{i^T} L^{\dagger} p^{j} \\ K_{ii} &= 1 \quad \forall i \\ K &\succeq 0 \end{aligned} \tag{3.16}$$

3.7 Computational results

3.7.1 One commodity

Although a substantial fraction of spectral graph theory applications deal directly or indirectly with NP-hard combinatorial optimization problems, we first focus on the single commodity case, which for the most part falls within the scope of linear programming and faster algorithms [4]. Our motivation comes from the amenability of eigenvalues to certain techniques not shared by linear and semidefinite programming, e.g. perturbation theory [116, 122].

We study the proximity of q to three variations of μ^r from Section 3.4.3 as functions of size and edge density. The three eigenvalues considered are μ^s (3.8), μ^{δ^z}, and μ^{δ^X} (3.7), where z is the vertex of largest degree and X is the minimizer of q. Relative error, defined $e(x) = |1 - x/q|$, is averaged over 1,000 randomly generated, 100-vertex flow networks with unit capacities, which are generated as follows. An Erdős-Rényi random graph with edge formation probability p_{ER} is sampled [52]; since p_{ER} directly determines the expected number of edges, we use it as a parametrization of edge density. If the graph is disconnected, a new one is drawn, since q and μ^r are trivially zero in this case. For each graph, a random vector p of supplies and demands is drawn from the normal distribution $\mathcal{N}(\mathbf{0}, I)$, and then $\sum_v p_v/n$ is subtracted from each element so that $\sum_v p_v = 0$.

Tables 3.1 and 3.2 summarize the results. $e\left(\mu^{\delta^z}\right)$ increases gradually, and $e\left(\mu^s\right)$ and $e\left(\mu^{\delta^X}\right)$ tend towards the same value, approximately approaching 0.12 from above and below, respectively. As p_{ER} is increased, $e\left(\mu^{\delta^z}\right)$ increases, but $e\left(\mu^s\right)$ and $e\left(\mu^{\delta^X}\right)$

decrease. We can see why this is so for $e\left(\mu^{\delta^X}\right)$ by applying a basic result from spectral graph theory. On a complete graph, $\lambda_1 = n/(n-1)$, and Theorem 2 reduces to $q \geq \mu^{\delta^X} \geq q\sqrt{\text{vol}(X)/2(n-1)^2}$. It is common in this case for X to contain all but a few vertices; when $|X| = n-1$, the lower bound is $q/\sqrt{2}$. μ^s, which did not exceed q in any trial, also exhibits error decreasing with p_{ER}.

Table 3.1: Mean relative errors of each eigenvalue on single-commodity networks with $p_{ER} = 10/n$ as a function of n.

n	100	200	300
$e\left(\mu^s\right)$	0.14	0.13	0.12
$e\left(\mu^{\delta^z}\right)$	0.54	0.58	0.60
$e\left(\mu^{\delta^X}\right)$	0.11	0.12	0.12

Table 3.2: Mean relative errors of each eigenvalue on single-commodity, 100-vertex networks as a function of p_{ER}.

p_{ER}	1/10	1/2	9/10
$e\left(\mu^s\right)$	0.14	0.085	0.084
$e\left(\mu^{\delta^z}\right)$	0.54	0.70	0.73
$e\left(\mu^{\delta^X}\right)$	0.11	0.013	0.0016

3.7.2 Multiple commodities

We now examine the quality of the relaxation (3.15) as a function of the number of commodities m and the number of vertices per commodity n_c. In each case, 100 30-vertex flow networks were randomly sampled as in the previous example with $p_{ER} = 1/2$, and mean relative error was computed for μ^{δ^z}, its semidefinite relaxation, $\tilde{\mu}^{\delta^z}$, and the corresponding rounding approximation to q, $\tilde{q}$. The vertices associated with each commodity were randomly assigned with uniform probability. Semidefinite programs were solved using the convex optimization tool CVX [65] and solver SeDuMi [117].

Tables 3.3 and 3.4 show that as both m and n_c are increased, the tightness of the eigenvalue and semidefinite bounds do not change significantly, but the ultimate approximation error of $\tilde{q}$ increases.

Table 3.3: Mean relative errors on five-commodity per node, 30-vertex networks as a function of m.

m	4	8	12
$e(\tilde{q})$	0.023	0.045	0.089
$e(\tilde{\mu}^{\delta^z})$	0.46	0.47	0.46
$e(\mu^{\delta^z})$	0.46	0.47	0.45

Table 3.4: Mean relative errors on 10-commodity, 30-vertex networks as a function of n_c.

n_c	10	20	30
$e(\tilde{q})$	0.066	0.12	0.19
$e(\mu^{\delta^z})$	0.46	0.42	0.39
$e(\tilde{\mu}^{\delta^z})$	0.47	0.43	0.40

3.8 Application: Stochastic flow networks

Probabilistic modeling provides a natural means for handling inherent uncertainty, yet few approaches exist outside of Monte Carlo simulation for stochastic flow networks; see [77, 104]. Of prime importance is feasibility: can a given network deliver the supplies at the sources to sink demands, and, moreover, what is the probability it can do so under stochastic conditions?

In this section we investigate the distribution of μ^z when the vertex flows are stochastic. Ideally, one would want the exact distribution of μ^z. If we approach the problem using finite random matrix theory [48, 98], even in the case of deterministic capacities we inevitably must find a diagonal matrix F^z associated with a given set of eigenvalues. This is known as a multiplicative inverse eigenvalue problem, and must be solved numerically, e.g. using a Newton's method based procedure [32]. Moreover, a given set of eigenvalues can correspond to as many as $n!$ diagonal matrices F^z [55], and so, given the nature of the underlying problem, neither an analytical expression or an efficient numerical procedure seem likely to exist for random flows, let alone random capacities. We instead consider two approximate approaches: bounds using the eigenvalue inequalities of Weyl, and a scaled approximation using perturbation theory. Unfortunately, in all but contrived cases the bounds of this section are impractically loose; they are included here however for thoroughness.

3.8.1 Bounds using Weyl's theorem

When only the vertex flows are random, we can use Weyl's theorem [71] to develop analytical expressions for the probability inequality

$$\text{prob}(\mu^z \geq \beta) \leq \text{prob}(q \geq \beta) \leq \text{prob}(\mu^z \geq \alpha\beta), \qquad \alpha = \sqrt{\frac{\lambda_G d_z}{2\text{vol}\,(V(G))}}. \tag{3.17}$$

The bound follows from Theorem 1 and the fact that if events A and B both occupy the same sample space and $A \rightarrow B$, then $\text{prob}(B) \geq \text{prob}(A)$. Assume that vertex z conserves flow, and that the rest are drawn from the $n-1$ dimensional multivariate distribution $\text{prob}(p)$; vertex z is typically referred to as the swing bus or slack node. Let L^z and P^z be L and P each with row and column z removed.

The condition $-L^z \preceq \gamma P^z \preceq L^z$, $\gamma \geq 0$ is equivalent to the positive definiteness of the matrices $L^z + \gamma P^z$ and $L^z - \gamma P^z$. We approximate this condition using the following theorem by Weyl [71]:

Theorem 3. *(Weyl) Let A and B be Hermitian matrices with eigenvalues $a_1 \leq \cdots \leq a_n$ and $b_1 \leq \cdots \leq b_n$, and let $c_1 \leq \cdots \leq c_n$ be those of $A+B$. Then*

$$a_{i-j+1} + b_j \leq c_i, \qquad j = 1, ..., i, \tag{3.18}$$

and

$$c_i \leq a_{i+j} + b_{n-j}, \qquad j = 0, ..., n-i. \tag{3.19}$$

Let $B^+ = L^z + \gamma E[P^z]$ and $B^- = L^z - \gamma E[P^z]$, and let $\delta_1^+ \leq \cdots \leq \delta_{n-1}^+$ and $\delta_1^- \leq \cdots \leq \delta_{n-1}^-$ be their eigenvalues. Let $\tilde{P} = P^z - E[P^z]$, and let $\tilde{p}_1 \leq \cdots \leq \tilde{p}_{n-1}$ be its diagonal elements. From (3.18) we have

$$\begin{aligned} \text{prob}\,(\mu^z \geq \gamma) &= \text{prob}\left(B^+ + \gamma\tilde{P} \succeq 0 \bigcap B^- - \gamma\tilde{P} \succeq 0\right) \\ &\geq \text{prob}\left(\delta_1^+ + \gamma \min_i \tilde{p}_i \geq 0 \bigcap \delta_1^- - \gamma \max_i \tilde{p}_i \geq 0\right) \\ &= \text{prob}\left(\bigcap_i -\delta_1^+ \leq \gamma\tilde{p}_i \leq \delta_1^-\right). \end{aligned} \tag{3.20}$$

We bound prob $(\mu^z \geq \gamma)$ from above using (3.19). If $B^+ + \gamma\tilde{P}$ and $B^- - \gamma\tilde{P}$ are positive definite, then

$$0 \leq \min_j \delta_j^+ + \gamma\tilde{p}_{n-j}, \qquad j = 1, ..., n-1, \tag{3.21}$$

and

$$0 \leq \min_j \delta_j^- - \gamma\tilde{p}_j, \qquad j = 1, ..., n-1, \tag{3.22}$$

which are equivalent to

$$\bigcap_j -\delta_{n-j}^+ \leq \gamma\tilde{p}_j \leq \delta_j^-. \tag{3.23}$$

By relaxing (3.23), we can disregard the ordering of the $\tilde{p}_j$ and obtain

$$\text{prob}\,(\mu^z \geq \gamma) \leq \text{prob}\left(\bigcap_j -\delta_n^+ \leq \gamma\tilde{p}_j \leq \delta_n^-\right). \tag{3.24}$$

We can construct sharper upper bounds by imposing assumptions on the density of p. Using the law of total probability, prob$(\mu^z \geq \gamma)$ is bounded above by

$$\text{prob}(\mu^z \geq \gamma) \leq \sum_S \text{prob}\left(\bigcap_j -\delta_{n-j}^+ \leq \gamma\tilde{p}_{S(j)} \leq \delta_j^- \bigcap S\right), \tag{3.25}$$

where S is a permutation of the indices $1, ..., n-1$. If the f_i have overlapping sample spaces, dependencies make (3.25) difficult to evaluate analytically. We consider a special case in which (3.25) simplifies dramatically. Assume that the $\tilde{p}_i$ can be organized into groups such that all $\tilde{p}_i$ in a particular group have the same distribution, and the distributions different groups do not overlap. Let the index sets be $T_1, ..., T_m$, ordered according to increasing sample spaces. Let S_k be the set of orderings for index set T_k, and let the $S \ni S_k$ be indexed S_k^l, $l = 1, ..., |T_k|!$. We can then rewrite (3.25) as

$$\text{prob}(\mu^z \geq \gamma) \leq \prod_k \text{prob}\left(\bigcup_{S \ni S_k} \bigcap_{j \ni T_k} -\delta_{n-j}^+ \leq \gamma\tilde{p}_{S_k^l(j)} \leq \delta_j^-\right) \tag{3.26}$$

Let R^m be the set of all size m subsets of $\{1, ..., |T_k|!\}$. Repeatedly applying the

identity $\text{prob}(A \cup B) = \text{prob}(A) + \text{prob}(B) - \text{prob}(A \cap B)$, we eventually obtain

$$\text{prob}(\mu^z \geq \gamma) \leq \prod_k \sum_{m=1}^{|T_k|!} (-1)^{m+1} \sum_{R \ni R_m} \text{prob}\left(\bigcap_{l \ni R} \bigcap_{j \ni T_k} -\delta_{n-j}^+ \leq \gamma \tilde{p}_{S_k^l(j)} \leq \delta_j^- \right). \quad (3.27)$$

3.8.2 Approximation using perturbation theory

We can approximate $\text{prob}(\mu^z \geq \gamma)$ using standard eigenvalue perturbation theory [122]. This formulation also allows us to consider uncertainty in graph structure, the interpretation of which we discuss later in this subsection. We consider the reciprocal eigensystem: we know that $\mu^z \geq \gamma$ if the largest magnitude eigenvalue of $(\gamma P^z, L^z)$ is in the interval $[-1, 1]$. Let $\nu_1, ..., \nu_{n-1}$ be the eigenvalues of $(E[P^z], E[L^z])$ ordered by decreasing magnitude, and $x_1, ..., x_{n-1}$ be the corresponding eigenvectors normalized about $E[L^z]$. Again let $\tilde{P}^z = P^z - E[P^z]$ with diagonal elements $\tilde{p}_i$, $i = 1, ..., n-1$. Also let $\tilde{L}^z = L^z - E[L^z]$ with elements $\tilde{l}_{ij}$, $i = 1, ..., n-1$, $j = 1, ..., n-1$. If we regard $\tilde{L}^z$ and $\tilde{P}$ to be respective perturbations to $E[L^z]$ and $E[P^z]$, we have the following approximation:

$$\text{prob}\left(\mu^z \geq \gamma\right) \approx \text{prob}\left(\bigcap_{i=1}^{t} -1/\gamma \leq \nu_i + x_i^T \left(\tilde{P}^z + \nu_i \tilde{L}^z \right) x_i \leq 1/\gamma \right), \quad (3.28)$$

where t is can be any number from 1 and $n-1$. Equation (3.28) approximates the probability that the t largest magnitude eigenvalues remain in $[-1, 1]$. When $t = n-1$, this can be an intractably high dimensional integral; however, noting that there are often only a few large magnitude eigenvalues to a given pencil, a highly accurate, easily computable approximation is obtained by setting t to a much smaller number.

Equation (3.28) involves a weighted sum of random variables. It is straightforward to evaluate when each variable is Gaussian, but other types are not easily approached. For example, one might wish to model thermal effects on line capacity in a power grid using exponential random variables, or even line failures with Bernoulli random variables. Unfortunately neither of these cases have analytical expressions. In Section 3.8.2 we focus our attention on Gaussian uncertainty exclusively in the supplies and

demands.

We note one apparently applicable distribution: the half-normal distribution, which is one side of a zero mean Gaussian distribution. This may be a reasonable approach to modeling stochastic capacity degradation, which results in exclusively changes to line capacity. Weighted sums of half-normal random variables remain half-normal, and hence admit convenient analytical expressions.

Estimating prob$(q \geq \gamma)$

The preceding constructions are unfortunately far from sharp enough to reliably estimate prob$(q \geq \gamma)$. Theorem 1 suggests a method by which to construct better estimates: since μ^z is bounded above and below by linear factors of q, assume that prob$(q \geq \gamma)$ has a shape similar to that of prob$(\mu^z \geq \gamma)$. Let $\theta = \bar{q}/\bar{\mu}^z$, where the overbar indicates evaluation at mean values. We then can estimate prob$(q \geq \gamma)$ with prob$(\theta\mu^z \geq \gamma)$ and the formulas of the previous section.

The accuracy of this approximation depends on how close the distribution of μ^z is to q and the accuracy of the perturbation. The former seems to degrade with growing network size, and the perturbation, as is to be expected, degrades as variance grows.

Example: reliability assessment of a power system

As a potential application of perturbations to μ^z, we consider reliability analysis of electric power systems. The probability a network flow approximation to a transmission system is feasible is a well-known quantification of reliability, and there have been efforts toward incorporating such a measure into design methodologies [31]. However, formulations are typically limited to analytical calculation of the probability load exceeds demand, without regard for network constraints, or rely on expensive Monte Carlo simulation of load flow [20]. The analytical approximations of the previous subsection offer an efficient circumvention of Monte Carlo simulation while retaining information about network structure and capacity; specifically, if uncertainty is Gaussian, we may use the analytical approximation (3.28) with the shift suggested above as a proxy for Monte-Carlo simulation.

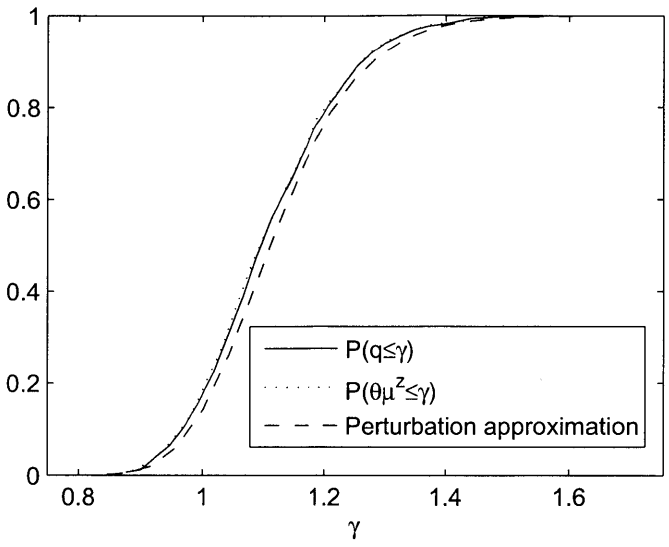

Figure 3-2: IEEE 118 bus test system feasibility pdf's. Increasing along the γ-axis implies 'higher' feasibility.

We apply our approximations to the IEEE 118 bus test system, a standard testbed in electric power system design and analysis [2]. Loads and generation are assumed to be at their maximum values, with the designated swing bus balancing flow. Edge capacities are uniformly 500, and generation, load, and topology are as in [2].

Supplies and demands, which here represent generation and loads, are drawn from a joint normal distribution with the following covariance structure. Weekly data from [67] indicates that the standard deviation of the loads is approximately ten percent, and so we set the standard deviation of each bus i to $\sigma_i = \bar{p}_i/10$, where $\bar{p}_i$ is the mean supply or demand at node i. The covariance between any two loads is zero, as is that between any two generators. Since we expect generation to track load, we set the covariance of a load bus i and a generator bus j to be $\sigma_{ij}^2 = \bar{p}_i\bar{p}_j/(100n_L)$, where n_L is the number of load buses.

The resulting cumulative distributions are shown in Fig. 3-2. The 'exact' (1000 Monte Carlo trials) probabilities of feasibility prob($q \geq 1$) and prob($\theta\mu \geq 1$) are respectively 0.85 and 0.86, and the probability estimated by the fifth-order perturbation approximation is 0.86.

The point at which the curves in Fig. 3-2 cross one on the γ axis is the probability the network will be infeasible. The shifted eigenvalue distrubution nearly overlaps the true feasibility distribution, and the error between the perturbation approximation and the true distribution is approximately one percent. This is a particularly accurate instance, but unfortunately such performance cannot be guaranteed in general.

3.9 Summary

We have defined a class of Laplacian matrix pencils and a new cut parameter for undirected, multicommodity flow networks. The parameter, which is a generalization of the sparsest cut, bounds the smallest magnitude eigenvalue of each pencil via a Cheeger-like inequality. The eigenvalue is used to formulate semidefinite relaxations, the quality of which is assessed in computational examples.

There are a number of potential venues for further development. The most obvious is the extension to directed flow networks; a Laplacian and Cheeger inequality exist for irreversible Markov chains [34], but the formulation implicitly normalizes edge weights, precluding an edge capacity interpretation. Better relaxation constraints, which do not necessarily correspond to eigenvector orthogonality conditions, are likely to exist. To this end, flow network versions of other spectral graph theory results, e.g. Poincare and Sobolev inequalities [33,42], may be useful in devising and perhaps bounding them. The distributions of μ^r and γ under random sources and sinks have many applications, for example an electric power grid with intermittent wind or solar generation [123]; approximate formulations have been derived, but more reliable estimates are necessary before practical applicability is attained.

Chapter 4

Transmission system planning

4.1 Introduction

Static transmission system planning is a network design problem in which lines are selected from a candidate set to meet certain physical requirements while minimizing investment and operational costs [88,107]. Linearized or 'DC' power flow is a standard simplification of AC power flow [124], which is usually too computationally intensive a representation of electrical physics for usage in optimization; only recently has this problem been approached in full [106]. For network design problems in which the existence of a line may be a variable, even linearized power flow becomes nonlinear, and furthermore, non-convex.

Current approaches to can be divided into two classes: metaheuristics [105] and classical algorithms [5, 107]. This work falls among the latter, the primary focus of which is circumventing the non-convexity of DC transmission system planning. This has traditionally been accomplished through linear relaxations, namely the so called transportation and disjunctive models [107].

Relaxed solutions such as those from the hybrid and disjunctive models are often infeasible for the original problem, but can contain a significant portion of the true optimal solution, thus reducing the size of the original problem, which may be intractable when approached directly [107]. Furthermore, the distance to feasibility is often slight, and thus the chance of obtaining an optimal or near optimal solution

through modification to a relaxed solution is often higher than when attempting to solve the original problem, which may have many local minima. Later in this chapter we elaborate on how a relaxed solution may be used to obtain feasible solutions within a nonlinear programming approach.

We apply the lift-and-project relaxations for polynomial optimization problems [85, 111] to transmission system planning. The approach is broadly applicable; we employ it here with the intention of both formulating new models and illustrating its potential for usage in power system optimization. First, we approach the DC power flow case and obtain a hierarchy of linear models, which includes the hybrid transportation [68] and disjunctive [21, 66, 110, 121] models, the latter of which we make more flexible. The relaxation is then applied to the full AC case, yielding a linear AC model which to our knowledge is the first of its kind.

The DC and AC models are tested on several standard examples from the transmission system planning literature. The new DC models demonstrate improved efficiency, and the AC models compare well with existing nonlinear approaches while retaining the efficiency of linear DC models. We also introduce a new benchmark test case based on the all-electric ship [44], a prototypical micro-grid design application, for which the disjunctive and transportation models are entirely unsuitable, as noted above.

4.2 DC power flow

4.2.1 Network design

In the standard DC load flow network design problem, we are given the following additional parameters: a line investment vector c, a vector of generation and demand p, normalized susceptances b, and normalized flow limits $\overline{f}$. Also given are the number of lines present in the existing network, η^0, and the number of additional lines which may be constructed, $\overline{\eta}$. Let Γ denote the set of buses, Ω_0 the set of existing lines, and Ω the set of candidate lines. We follow the notational conventions that unless

otherwise specified, single subscripts denote members of Γ, double subscripts members of Ω, and $i \sim j$ summation over $\Omega_0 \cup \Omega$.

(2.4) is incorporated into a network design framework by making the susceptances b linear functions of the line quantities η^0 and η. The nonlinear DC load flow network design problem is given by

$$\text{NLDC} \quad \min_{\theta,\eta,f} \quad \sum_{i\sim j} c_{ij}\eta_{ij} \tag{4.1}$$

$$\text{s.t.} \quad \sum_{j:i\sim j} f_{ij} = p_i \tag{4.2}$$

$$f_{ij} - b_{ij}(\eta^0_{ij} + \eta_{ij})(\theta_i - \theta_j) = 0 \qquad (i,j) \in \Omega_0 \cup \Omega \tag{4.3}$$

$$|f_{ij}| \leq (\eta^0_{ij} + \eta_{ij})\overline{f}_{ij} \tag{4.4}$$

$$0 \leq \eta_{ij} \leq \overline{\eta}_{ij}, \qquad \eta_{ij} \in \mathbb{N} \tag{4.5}$$

where the variables θ are bus angles, η candidate lines, and f power flows. Constraints (4.1), (4.2), (4.4), and (4.5) are standard flow network design constraints [95]. The main difficulty in using the above formulation is the additional constraint (4.3): it is bilinear and hence non-convex.

4.2.2 Linear models

We first reformulate NLDC in a way which, upon application of the relaxation of [111], leads to a class of disjunctive models. Eliminate the variables f by substitution of constraint (4.3), and rewrite NLDC

$$\text{NLDCS} \quad \min_{\theta,\eta} \quad \sum_{i\sim j} c_{ij}\eta_{ij} \tag{4.6}$$

$$\text{s.t.} \quad \sum_{j:i\sim j} b_{ij}\left(\eta^0_{ij} + \eta_{ij}\right)(\theta_i - \theta_j) = p_i \tag{4.7}$$

$$b_{ij}|\theta_i - \theta_j| \leq \overline{f}_{ij} \qquad (i,j) \in \Omega_0 \tag{4.8}$$

$$b_{ij}\eta_{ij}|\theta_i - \theta_j| \leq \overline{f}_{ij}\eta_{ij} \tag{4.9}$$

$$0 \leq \eta_{ij} \leq \overline{\eta}_{ij}, \qquad \eta_{ij} \in \mathbb{N} \tag{4.10}$$

(4.9) is required to preserve the equivalence of NLDCS and NLDC. If (4.8) alone was enforced over all the lines, artificial constraints on angles would arise between buses that were not directly connected.

We derive an additional constraint set which is implicit in (4.8), but leads to a tighter relaxation. Consider a line $(i,j) \in \Omega$, and let s_{ij} be a path connecting i and j through Ω_0. Summing constraint (4.8) along s_{ij} and multiplying by b_{ij} gives

$$b_{ij}\,|\theta_i - \theta_j| \leq M_{ij} \qquad (i,j) \in \Omega. \tag{4.11}$$

where $M_{ij} = b_{ij} \sum_{(k,l)\in s_{ij}} \overline{f}_{kl}/x_{kl}$. Clearly (4.11) is sharpest when s_{ij} is the shortest path through the graph induced by Ω_0 with edge weights $\overline{f}_{kl}/x_{kl}$, $(k,l) \in \Omega_0$, which matches the result stated in [21]. If no path between the nodes i and j exists in Ω_0, s_{ij} can be set to the longest path through the existing and candidate networks [21]. This however is an NP-hard calculation that contributes little accuracy; M_{ij} can instead be set to some sufficiently large number, e.g. $\sum_{(i,j)\in\Omega\cup\Omega_0} \overline{f}_{ij}/b_{ij}$.

We now apply the relaxation to NLDCS with constraint (4.11). We develop a second-order linearization by introducing the variable $\zeta_{ij} = b_{ij}\eta_{ij}(\theta_i - \theta_j)$, and then constraining ζ with (4.9) and products of (4.8), (4.10), and (4.11). For example, we obtain constraint (4.17) by multiplying $M_{ij} - b_{ij}|\theta_i - \theta_j|$ from (4.11) with $\overline{\eta}_{ij} - \eta_{ij}$ from (4.10), and then substituting ζ_{ij} wherever $b_{ij}\eta_{ij}(\theta_i - \theta_j)$ appears.

We thus have the following relaxation:

$$\text{LDC} \quad \min_{\theta,\eta,\zeta} \quad \sum_{i\sim j} c_{ij}\eta_{ij} \tag{4.12}$$

$$\text{s.t.} \quad \sum_{j\sim i} \zeta_{ij} + b_{ij}\eta^0_{ij}(\theta_i - \theta_j) = p_i \tag{4.13}$$

$$b_{ij}|\theta_i - \theta_j| \leq \overline{f}_{ij} \qquad (i,j) \in \Omega_0 \tag{4.14}$$

$$0 \leq \eta_{ij} \leq \overline{\eta}_{ij} \tag{4.15}$$

$$|\zeta_{ij}| \leq \min\{M_{ij}, \overline{f}_{ij}\}\eta_{ij} \tag{4.16}$$

$$\left|\zeta_{ij} - b_{ij}\overline{\eta}_{ij}\,(\theta_i - \theta_j)\right| \leq M_{ij}\left(\overline{\eta}_{ij} - \eta_{ij}\right) \tag{4.17}$$

$$0 \leq \eta_{ij} \leq \overline{\eta}_{ij}, \qquad \eta_{ij} \in \mathbb{N} \tag{4.18}$$

For comparison, the original disjunctive model, which only admits a binary formulation, is

$$\text{DM} \quad \min_{\theta,\eta,\zeta} \quad \sum_{i\sim j} c_{ij} \sum_{k} \eta_{ij}^{k} \tag{4.19}$$

$$\text{s.t.} \quad \sum_{j\sim i} b_{ij}\eta_{ij}^{0}(\theta_i - \theta_j) + \sum_{k} \zeta_{ij}^{k} = p_i \tag{4.20}$$

$$b_{ij}|\theta_i - \theta_j| \leq \overline{f}_{ij} \qquad (i,j) \in \Omega_0 \tag{4.21}$$

$$|\zeta_{ij}^{k}| \leq \overline{f}_{ij}\eta_{ij}^{k} \tag{4.22}$$

$$\left|\zeta_{ij}^{k} - b_{ij}\left(\theta_i - \theta_j\right)\right| \leq M_{ij}\left(1 - \eta_{ij}^{k}\right) \tag{4.23}$$

$$\eta_{ij}^{k} \in \{0,1\} \qquad k = 1,...,\overline{\eta}_{ij} \tag{4.24}$$

DM and LDC are quite similar; indeed LDC can be straightforwardly transformed to a binary problem which is identical to DM save constraint (4.22), which is looser than (4.16), its counterpart in LDC. Moreover, line quanta may be aggregated in any fashion, so that a particular discrete variable may represent any number of candidate lines between one and $\overline{\eta}_{ij}$. From this perspective, DM and LDC represent opposing ends of a spectrum, which in general becomes less accurate and more efficient as one moves from $\overline{\eta}_{ij}$ binary variables to a single integer variable per line.

We remark that if we apply the substitution $\zeta_{ij} = b_{ij}\eta_{ij}(\theta_i - \theta_j)$ to NLDCS without forming any constraint products, the flows are only constrained by line capacities, and we obtain a hybrid model [107] in which flows in existing lines are governed by DC power flow, and in new lines by the network flow [4, 76].

4.3 AC power flow

There has been little work to date on transmission system planning using AC power flow. A notable recent approach is [106], in which a full AC model is solved by an interior point method in tandem with a constructive heuristic algorithm. We now derive linear models for AC transmission system planning which are similar in structure and size to the disjunctive models of the previous section. Solutions can be

used in the same fashion as those from linear DC models, and hence the new models mark a significant improvement in the overall design procedure via removal of the DC approximation.

Let s, v, and y respectively denote complex powers, voltages and admittances, and let $\underline{p}$, $\overline{p}$, $\underline{q}$, and $\overline{q}$ respectively be lower and upper real and reactive power limits, e.g. if bus i is a purely real load, $\underline{p}$ and $\overline{p}$ are both equal to the load value, and $\underline{q} = \overline{q} = 0$. The remaining notation is identical to the previous section. The basic AC power flow model is then given by

$$\text{NLAC} \quad \min_{\eta,s,v} \quad \sum_{i\sim j} c_{ij}\eta_{ij} \tag{4.25}$$

$$\text{s.t.} \quad s_{ij} = \left(\eta^0_{ij} + \eta_{ij}\right)\left(v_i v_i^* y_{ij}^* - v_i v_j^* y_{ij}^*\right) \tag{4.26}$$

$$\underline{p}_i \leq \text{Re}\sum_j s_{ij} \leq \overline{p}_i \tag{4.27}$$

$$\underline{q}_i \leq \text{Im}\sum_j s_{ij} \leq \overline{q}_i \tag{4.28}$$

$$\underline{v}_i \leq |v_i| \leq \overline{v}_i \tag{4.29}$$

$$|s_{ij}| \leq \left(\eta^0_{ij} + \eta_{ij}\right)\overline{s}_{ij} \qquad (i,j) \in \Omega_0 \cup \Omega \tag{4.30}$$

$$0 \leq \eta_{ij} \leq \overline{\eta}_{ij}, \qquad \eta_{ij} \in \mathbb{N} \tag{4.31}$$

Note that although line variables and parameters are non-directional, i.e. $\eta_{ij} = \eta_{ji}$, $\overline{s}_{ij} = \overline{s}_{ji}$ and so on, sending and receiving power flows s_{ij} and s_{ji} are not.

4.3.1 Linear models

We first must rewrite NLAC in terms of real, polynomial constraints so we may begin to build a relaxation. Let $y = g + jb$, $v = w + jx$, $s = p + jq$, and let $b^s = b + b^{sh}$, where b^{sh} is the line shunt susceptance. NLAC is then given by

$$\text{NLACS} \quad \min_{\eta,p,q,w,x} \quad \sum_{i\sim j} c_{ij}\eta_{ij} \tag{4.32}$$

$$\text{s.t.} \quad p_{ij} = \left(\eta^0_{ij} + \eta_{ij}\right)\left(b_{ij}(w_i x_j - w_j x_i)\right.$$
$$\left. -g_{ij}(x_i x_j + w_i w_j) + g_{ij}(w_i^2 + x_i^2)\right) \tag{4.33}$$

$$q_{ij} = \left(\eta_{ij}^0 + \eta_{ij}\right)\left(g_{ij}(w_i x_j - w_j x_i)\right.$$
$$\left. + b_{ij}(x_i x_j + w_i w_j) - b_{ij}^s(w_i^2 + x_i^2)\right) \tag{4.34}$$

$$\underline{p}_i \leq \sum_j p_{ij} \leq \overline{p}_i \tag{4.35}$$

$$\underline{q}_i \leq \sum_j q_{ij} \leq \overline{q}_i \tag{4.36}$$

$$\underline{v}_i^2 \leq w_i^2 + x_i^2 \leq \overline{v}_i^2 \tag{4.37}$$

$$\sqrt{p_{ij}^2 + q_{ij}^2} \leq \left(\eta_{ij}^0 + \eta_{ij}\right)\overline{s}_{ij}$$
$$(i,j) \in \Omega_0 \cup \Omega \tag{4.38}$$

$$0 \leq \eta_{ij} \leq \overline{\eta}_{ij}, \qquad \eta_{ij} \in \mathbb{N} \tag{4.39}$$

Constraint (4.38) represents a slight obstacle: although it can be expressed polynomially, fourth order products of the original variables are involved, rendering the size of the resulting relaxation impractically large. We instead approximate it so that p and q are involved linearly. A few options are apparent; for example, introduce the constants τ^1 and τ^2, and replace (4.38) with

$$\tau_{ij}^1 |p_{ij}| + \tau_{ij}^2 |q_{ij}| \leq \left(\eta_{ij}^0 + \eta_{ij}\right)\overline{s}_{ij} \tag{4.40}$$

Notice, for example, that by setting τ^1 and τ^2 to one, we obtain a more conservative constraint than (4.38), which is no longer a relaxation, while by setting τ^2 to zero, we relax (4.38) by only limiting the flow of active power. Although we have opted to approximate (4.38) with a single constraint, any piecewise linear approximation can be accommodated.

Define the new variables:

$$\begin{aligned}
\alpha_i &= w_i^2 + x_i^2 \\
\delta_{ij} &= \eta_{ij}\left(w_i^2 + x_i^2\right) \\
\mu_{ij} &= b_{ij}(w_i x_j - w_j x_i) - g_{ij}(x_i x_j + w_i w_j) + g_{ij}(w_i^2 + x_i^2) \\
\nu_{ij} &= g_{ij}(w_i x_j - w_j x_i) + b_{ij}(x_i x_j + w_i w_j) - b_{ij}^s(w_i^2 + x_i^2)
\end{aligned}$$

$$\begin{aligned}
\phi_{ij} &= \eta_{ij}\left(b_{ij}(w_i x_j - w_j x_i) - g_{ij}(x_i x_j + w_i w_j) + g_{ij}(w_i^2 + x_i^2)\right) \\
\psi_{ij} &= \eta_{ij}\left(g_{ij}(w_i x_j - w_j x_i) + b_{ij}(x_i x_j + w_i w_j) - b_{ij}^s(w_i^2 + x_i^2)\right)
\end{aligned}$$

Certain symmetries are present in these variables, which we use to form additional constraints. Before showing them, we first give a brief example illustrating why they exist; suppose y_{ij} is substituted for the product $x_i x_j$; the implicit constraint $y_{ij} = y_{ji}$ follows from the fact that $x_i x_j = x_j x_i$. The following constraints are similarly formed by taking linear combinations of (4.33) and (4.34) and performing the above substitutions to relate new variables from i to j and j to i:

$$\begin{aligned}
g_{ij}(\mu_{ij} - \mu_{ji}) - b_{ij}(\nu_{ij} - \nu_{ji}) &= \left(g_{ij}^2 + b_{ij}b_{ij}^s\right)(\alpha_i - \alpha_j) \\
b_{ij}(\mu_{ij} + \mu_{ji}) + g_{ij}(\nu_{ij} + \nu_{ji}) &= \left(g_{ij}b_{ij} - g_{ij}b_{ij}^s\right)(\alpha_i + \alpha_j) \\
g_{ij}(\phi_{ij} - \phi_{ji}) - b_{ij}(\psi_{ij} - \psi_{ji}) &= \left(g_{ij}^2 + b_{ij}b_{ij}^s\right)(\delta_{ij} - \delta_{ji}) \\
b_{ij}(\phi_{ij} + \phi_{ji}) + g_{ij}(\psi_{ij} + \psi_{ji}) &= \left(g_{ij}b_{ij} - g_{ij}b_{ij}^s\right)(\delta_{ij} - \delta_{ji})
\end{aligned}$$

Let Φ denote the set on which the variables μ, ν, ϕ, ψ, α, and δ satisfy these equalities. Forming constraints containing up to second-order terms and substituting the new variables, we have

$$\text{LAC} \quad \min_{\eta,\mu,\nu,\phi,\psi,\alpha,\delta} \quad \sum_{i\sim j} c_{ij}\eta_{ij} \tag{4.41}$$

$$\text{s.t.} \quad \{\mu,\nu,\phi,\psi,\alpha,\delta\} \in \Phi \tag{4.42}$$

$$\underline{p}_i \le \sum_j \eta_{ij}^0 \mu_{ij} + \phi_{ij} \le \overline{p}_i \tag{4.43}$$

$$\underline{q}_i \le \sum_j \eta_{ij}^0 \nu_{ij} + \psi_{ij} \le \overline{q}_i \tag{4.44}$$

$$\underline{v}_i^2 \le \alpha_i \le \overline{v}_i^2 \tag{4.45}$$

$$\underline{v}_i^2 \eta_{ij} \le \delta_{ij} \le \overline{v}_i^2 \eta_{ij} \tag{4.46}$$

$$\underline{v}_i^2\left(\overline{\eta}_{ij} - \eta_{ij}\right) \le \overline{\eta}_{ij}\alpha_i - \delta_{ij} \le \overline{v}_i^2\left(\overline{\eta}_{ij} - \eta_{ij}\right) \tag{4.47}$$

$$\tau_{ij}^1 |\mu_{ij}| + \tau_{ij}^2 |\nu_{ij}| \le \overline{s}_{ij} \qquad (i,j) \in \Omega_0 \tag{4.48}$$

$$\tau_{ij}^1 |\phi_{ij}| + \tau_{ij}^2 |\psi_{ij}| \leq \overline{s}_{ij} \eta_{ij} \tag{4.49}$$

$$\tau_{ij}^1 \left|\overline{\eta}_{ij}\mu_{ij} - \phi_{ij}\right| + \tau_{ij}^2 \left|\overline{\eta}_{ij}\nu_{ij} - \psi_{ij}\right| \leq \overline{s}_{ij} \left(\overline{\eta}_{ij} - \eta_{ij}\right) \qquad (i,j) \in \Omega_0 \tag{4.50}$$

$$0 \leq \eta_{ij} \leq \overline{\eta}_{ij}, \qquad \eta_{ij} \in \mathbb{N} \tag{4.51}$$

LAC is quite similar to LDC and the disjunctive model. μ and ϕ respectively represent active power flows in the existing and new networks, and μ and ϕ similarly represent reactive power flows. Constraint (4.50) is directly analogous to (4.17); unfortunately, it cannot be extended to lines not in the preexisting network, because (4.48) does not reduce to an expression with only i and j indices when summed along paths from i to j through Ω_0.

As with the disjunctive model, we are also able to formulate a binary version which is less efficient but more accurate:

$$\text{LACB} \qquad \min_{\eta,\mu,\nu,\phi,\psi,\alpha,\delta} \quad \sum_{i\sim j} c_{ij} \sum_k \eta_{ij}^k \tag{4.52}$$

$$\text{s.t.} \qquad \underline{p}_i \leq \sum_j \eta_{ij}^0 \mu_{ij} + \sum_k \phi_{ij}^k \leq \overline{p}_i \tag{4.53}$$

$$\underline{q}_i \leq \sum_j \eta_{ij}^0 \nu_{ij} + \sum_k \psi_{ij}^k \leq \overline{q}_i \tag{4.54}$$

$$\underline{v}_i^2 \leq \alpha_i \leq \overline{v}_i^2 \tag{4.55}$$

$$\underline{v}_i^2 \eta_{ij}^k \leq \delta_{ij}^k \leq \overline{v}_i^2 \eta_{ij}^k \tag{4.56}$$

$$\underline{v}_i^2 \left(1 - \eta_{ij}^k\right) \leq \alpha_i - \delta_{ij}^k \leq \overline{v}_i^2 \left(1 - \eta_{ij}^k\right) \tag{4.57}$$

$$\tau_{ij}^1 |\mu_{ij}| + \tau_{ij}^2 |\nu_{ij}| \leq \overline{s}_{ij} \qquad (i,j) \in \Omega_0 \tag{4.58}$$

$$\tau_{ij}^1 \left|\phi_{ij}^k\right| + \tau_{ij}^2 \left|\psi_{ij}^k\right| \leq \overline{s}_{ij} \eta_{ij}^k \tag{4.59}$$

$$\tau_{ij}^1 \left|\mu_{ij} - \phi_{ij}^k\right| + \tau_{ij}^2 \left|\nu_{ij} - \psi_{ij}^k\right| \leq \overline{s}_{ij} \left(1 - \eta_{ij}^k\right) \qquad (i,j) \in \Omega_0 \tag{4.60}$$

$$\eta_{ij}^k \in \{0,1\} \qquad k = 1, ..., \overline{k}_{ij} \tag{4.61}$$

Note that LAC has roughly two to four times the number of constraints in LDC, depending on the choice of τ^1 and τ^2; essentially, any system LDC or the hybrid model is applicable to is within the scope of LAC as well. The same parity exists for DM and LACB.

4.3.2 Semidefinite and second-order cone models

In [89], the standard constraints of AC optimal power flow are convexified via a semidefinite relaxation in the style of [60], as described in detail in Section 2.3. To summarize, the basic approach is to define a column vector X of the real and imaginary bus voltages w and x, and then substitute the symmetric matrix W for XX^T subject to the constraint $\text{rank}(W) = 1$ and $W \succeq 0$, where $\succeq$ denotes matrix semidefiniteness. Dropping the rank constraint yields the relaxation.

A dual formulation of the power flow equations is used in [89] to eliminate unnecessary variables; it is more convenient here to remain with the primal variables. The size of the positive semidefinite constraint $W \succeq 0$ can be alleviated by sparsifying W and instead using the relaxed condition

$$\begin{bmatrix} W_{i,i} & W_{i,j} & W_{i,i+n} & W_{i,j+n} \\ W_{j,i} & W_{j,j} & W_{j,i+n} & W_{j,j+n} \\ W_{i+n,i} & W_{i+n,j} & W_{i+n,i+n} & W_{i+n,j+n} \\ W_{j+n,i} & W_{j+n,j} & W_{j+n,i+n} & W_{j+n,j+n} \end{bmatrix} \succeq 0 \tag{4.62}$$

for each line (i, j). We denote the above submatrix ${}^{ij}W$, and substitute the 4×4 matrix Δ^{ij} for each instance of the product $\eta_{ij}{}^{ij}W$. In addition to symmetry, Δ^{ij} is implicitly constrained so that $\Delta^{ij}_{11} = \Delta^{ji}_{22}$, $\Delta^{ij}_{33} = \Delta^{ji}_{44}$, $\Delta^{ij}_{12} = \Delta^{ji}_{12}$, $\Delta^{ij}_{34} = \Delta^{ji}_{34}$, $\Delta^{ij}_{13} = \Delta^{ji}_{24}$, and $\Delta^{ij}_{14} = \Delta^{ji}_{23}$.

We then have the following mixed-integer semidefinite program:

$$\text{SDAC} \quad \min_{\eta,p,q,\phi,\psi,W,\Delta} \quad \sum_{(i,j)\in\Omega_0\cup\Omega} c_{ij}\eta_{ij} \tag{4.63}$$

$$\text{s.t.} \quad W \succeq 0 \quad \text{or} \quad {}^{ij}W \succeq 0 \tag{4.64}$$

$$0 \preceq \Delta^{ij} \preceq \overline{\eta}_{ij}{}^{ij}W \tag{4.65}$$

$$p_{ij} = g_{ij}(W_{i,i} + W_{i+n,i+n}) + b_{ij}(W_{i,j+n} - W_{j,i+n}) - g_{ij}(W_{i,j} + W_{i+n,j+n}) \tag{4.66}$$

$$q_{ij} = -b^s_{ij}(W_{i,i} + W_{i+n,i+n}) + g_{ij}(W_{i,j+n} - W_{j,i+n}) + b_{ij}(W_{i,j} + W_{i+n,j+n}) \tag{4.67}$$

$$\phi_{ij} = g_{ij}(\Delta^{ij}_{11} + \Delta^{ij}_{33}) + b_{ij}(\Delta^{ij}_{14} - \Delta^{ij}_{23}) - g_{ij}(\Delta^{ij}_{12} + \Delta^{ij}_{34}) \tag{4.68}$$

$$\psi_{ij} = -b^s_{ij}(\Delta^{ij}_{11} + \Delta^{ij}_{33}) + g_{ij}(\Delta^{ij}_{14} - \Delta^{ij}_{23}) + b_{ij}(\Delta^{ij}_{12} + \Delta^{ij}_{34}) \tag{4.69}$$

$$\underline{p}_i \leq \sum_j \eta^0_{ij} p_{ij} + \phi_{ij} \leq \overline{p}_i \tag{4.70}$$

$$\underline{q}_i \leq \sum_j \eta^0_{ij} q_{ij} + \psi_{ij} \leq \overline{q}_i \tag{4.71}$$

$$\underline{v}_i^2 \leq W_{i,i} + W_{i+n,i+n} \leq \overline{v}_i^2 \tag{4.72}$$

$$\underline{v}_i^2 \eta_{ij} \leq \Delta^{ij}_{11} + \Delta^{ij}_{33} \leq \overline{v}_i^2 \eta_{ij} \tag{4.73}$$

$$\underline{v}_j^2 \eta_{ij} \leq \Delta^{ij}_{22} + \Delta^{ij}_{44} \leq \overline{v}_j^2 \eta_{ij} \tag{4.74}$$

$$\underline{v}_i^2 \left(\overline{\eta}_{ij} - \eta_{ij}\right) \leq \overline{\eta}_{ij} \left(W_{i,i} + W_{i+n,i+n}\right) - \Delta^{ij}_{11} - \Delta^{ij}_{33} \leq \overline{v}_i^2 \left(\overline{\eta}_{ij} - \eta_{ij}\right) \tag{4.75}$$

$$\underline{v}_j^2 \left(\overline{\eta}_{ij} - \eta_{ij}\right) \leq \overline{\eta}_{ij} \left(W_{j,j} + W_{j+n,j+n}\right) - \Delta^{ij}_{22} - \Delta^{ij}_{44} \leq \overline{v}_j^2 \left(\overline{\eta}_{ij} - \eta_{ij}\right) \tag{4.76}$$

$$p_{ij}^2 + q_{ij}^2 \leq \overline{s}_{ij}^2 \qquad (i,j) \in \Omega_0 \tag{4.77}$$

$$\phi_{ij}^2 + \psi_{ij}^2 \leq \eta_{ij}^2 \overline{s}_{ij}^2 \tag{4.78}$$

$$\left(\overline{\eta}_{ij} p_{ij} - \phi_{ij}\right)^2 + \left(\overline{\eta}_{ij} q_{ij} - \psi_{ij}\right)^2 \leq \left(\overline{\eta}_{ij} - \eta_{ij}\right)^2 \overline{s}_{ij}^2 \qquad (i,j) \in \Omega_0 \tag{4.79}$$

$$0 \leq \eta_{ij} \leq \overline{\eta}_{ij}, \qquad \eta_{ij} \in \mathbb{N} \tag{4.80}$$

Using SDAC as a starting point, we can straightforwardly construct a second-order cone relaxation (SOCAC) via the fact that positivity of all two by two principal minors is a necessary condition for positive semidefiniteness [82]. The relaxation is thus obtained by replacing $W \succeq 0$ (or ${}^{ij}W \succeq 0$) and $\overline{\eta}_{ij}\Delta^{ij} \succeq {}^{ij}W$ with the second-

order cone constraints

$$
\begin{aligned}
&W_{i,i} \geq 0 \\
&W_{i+n,i+n} \geq 0 \\
&\Delta_{kk}^{ij} \geq 0
\end{aligned}
$$

$$
\begin{aligned}
&W_{i,j}^2 \leq W_{i,i} W_{j,j} \\
&W_{i,j+n}^2 \leq W_{i,i} W_{j+n,j+n} \\
&W_{i+n,j}^2 \leq W_{i+n,i+n} W_{j,j} \\
&W_{i+n,j+n}^2 \leq W_{i+n,i+n} W_{j+n,j+n}
\end{aligned}
$$

$$
\begin{aligned}
&{\Delta_{12}^{ij}}^2 \leq \Delta_{11}^{ij} \Delta_{22}^{ij} \\
&{\Delta_{14}^{ij}}^2 \leq \Delta_{11}^{ij} \Delta_{44}^{ij} \\
&{\Delta_{23}^{ij}}^2 \leq \Delta_{22}^{ij} \Delta_{33}^{ij} \\
&{\Delta_{34}^{ij}}^2 \leq \Delta_{33}^{ij} \Delta_{44}^{ij}
\end{aligned}
$$

$$
\begin{aligned}
&\left(\overline{\eta}_{ij} W_{i,j} - \Delta_{12}^{ij}\right)^2 \leq \left(\overline{\eta}_{ij} W_{i,i} - \Delta_{11}^{ij}\right) \left(\overline{\eta}_{ij} W_{j,j} - \Delta_{22}^{ij}\right) \\
&\left(\overline{\eta}_{ij} W_{i,j+n} - \Delta_{14}^{ij}\right)^2 \leq \left(\overline{\eta}_{ij} W_{i,i} - \Delta_{11}^{ij}\right) \left(\overline{\eta}_{ij} W_{j+n,j+n} - \Delta_{44}^{ij}\right) \\
&\left(\overline{\eta}_{ij} W_{i+n,j} - \Delta_{32}^{ij}\right)^2 \leq \left(\overline{\eta}_{ij} W_{j,j} - \Delta_{22}^{ij}\right) \left(\overline{\eta}_{ij} W_{i+n,i+n} - \Delta_{33}^{ij}\right) \\
&\left(\overline{\eta}_{ij} W_{i+n,j+n} - \Delta_{34}^{ij}\right)^2 \leq \left(\overline{\eta}_{ij} W_{i+n,i+n} - \Delta_{33}^{ij}\right) \left(\overline{\eta}_{ij} W_{j+n,j+n} - \Delta_{44}^{ij}\right)
\end{aligned}
$$

for each line (i, j). As with the linear models, it is straightforward to formulate more accurate but less efficient binary versions of both models.

4.4 Related problems of interest

Thus far we have focused on general AC systems. In this section we consider two specific variants arising from the all-electric ship and microgrids in general.

4.4.1 Direct current systems

DC distribution systems have received consideration for the electric ship [35], industrial applications [12], and microgrids [73], and give rise to an analogous transmission planning problem; however, in a DC system, assuming prescribed bus voltages v, the basic model is entirely linear without modification. Although it is straightforward, we include it here for completeness. Let f be a line current, and let r be line resistance. For conciseness we assume current generation and loading, but note that buses with prescribed power generation or consumption can be accommodated without sacrificing linearity. The DC distribution design model is given by

$$\text{DC} \quad \min_{\eta, f} \quad \sum_{i \sim j} c_{ij} \eta_{ij} \tag{4.81}$$

$$\text{s.t.} \quad \sum_{j : i \sim j} f_{ij} = p_i \tag{4.82}$$

$$r_{ij} f_{ij} - (\eta^0_{ij} + \eta_{ij})(v_i - v_j) = 0 \tag{4.83}$$

$$|f_{ij}| \leq (\eta^0_{ij} + \eta_{ij}) \overline{f}_{ij} \tag{4.84}$$

$$0 \leq \eta_{ij} \leq \overline{\eta}_{ij}, \qquad \eta_{ij} \in \mathbb{N} \tag{4.85}$$

4.4.2 Multiple scenarios

There are a number of extensions to transmission system planning which contain the basic formulation. In this section we discuss examples in the context of electric ship, to highlight that the developments in this chapter fit easily within such extensions. Unlike a terrestrial system, a ship may encounter multiple highly different sets of loads, each occurring independently, for example traveling at high speed and combat. Varying structural parameters also need to be taken into consideration in addressing failures through contingency analysis. A simple approach would be to simply optimize with each load bus consuming the maximum power over all scenarios; this however, may lead to highly conservative designs.

We can instead produce designs that are not overly conservative by creating constraints and variables for each scenario or contingency, and optimizing the same ob-

jective. Suppose we are given n_S scenarios, and for each scenario $k = 1, ..., n_S$ we have a set of parameters indicated by the superscript k. Using a separate set of variables for each set of power levels, we have the following multiple scenario transmission planning problem:

$$
\begin{aligned}
\text{MSAC} \quad & \min_{\eta, s^k, v^k} \quad \sum_{i \sim j} c_{ij} \eta_{ij} \\
\text{s.t.} \quad & s_{ij}^k = \left(\eta_{ij}^0 + \eta_{ij}\right)\left(v_i^k v_i^{k*} y_{ij}^{k*} - v_i^k v_j^{k*} y_{ij}^{k*}\right) \qquad \forall k \\
& \underline{p}_i^k \leq \mathrm{Re} \sum_j s_{ij}^k \leq \overline{p}_i^k \qquad \forall k \\
& \underline{q}_i^k \leq \mathrm{Im} \sum_j s_{ij}^k \leq \overline{q}_i^k \qquad \forall k \\
& \underline{v}_i^k \leq \left|v_i^k\right| \leq \overline{v}_i^k \qquad \forall k \\
& \left|s_{ij}^k\right| \leq \left(\eta_{ij}^0 + \eta_{ij}\right) \overline{s}_{ij}^k \qquad (i,j) \in \Omega_0 \cup \Omega, \forall k \\
& 0 \leq \eta_{ij} \leq \overline{\eta}_{ij}, \qquad \eta_{ij} \in \mathbb{N}
\end{aligned}
$$

From here, relaxations may be developed by identically applying the procedures of the previous section.

4.5 Design framework

As stated, an optimal solution to a relaxed problem is unlikely to be feasible for the original problem. In this section, we express precisely our comment from the Introduction to this chapter on making use of relaxed solutions. Suppose that η^r is a solution to the relaxation LAC, and we are interested in a good feasible solution to NLAC, since optimality is too much to ask for most realistically sized problems.

We then suggest reinforcing η^r via the following nonlinear model, which can be solved using any nonlinear approach, e.g. branch and bound with sequential quadratic

programming [18].

$$\text{NLACR} \quad \min_{\eta,s,v} \quad \sum_{i\sim j} c_{ij}\eta_{ij} \tag{4.86}$$

$$\text{s.t.} \quad s_{ij} = \left(\eta^0_{ij} + \eta^r_{ij} + \eta_{ij}\right)\left(v_i v_i^* y_{ij}^* - v_i v_j^* y_{ij}^*\right) \tag{4.87}$$

$$\underline{p}_i \le \mathrm{Re}\sum_j s_{ij} \le \overline{p}_i \tag{4.88}$$

$$\underline{q}_i \le \mathrm{Im}\sum_j s_{ij} \le \overline{q}_i \tag{4.89}$$

$$\underline{v}_i \le |v_i| \le \overline{v}_i \tag{4.90}$$

$$|s_{ij}| \le \left(\eta^0_{ij} + \eta^r_{ij} + \eta_{ij}\right)\overline{s}_{ij} \qquad (i,j) \in \Omega_0 \cup \Omega \tag{4.91}$$

$$0 \le \eta_{ij} \le \overline{\eta}_{ij}, \qquad \eta_{ij} \in \mathbb{N} \tag{4.92}$$

The solution $\eta^r + \eta^*$, where η^* is feasible for the above, is clearly feasible for NLAC. If η^r contains a substantial part of the true optimal solution, then the cost of NLACR landing in a local minimum is likely to be far less severe than with NLAC. Furthermore, if line limits $\overline{\eta}$ are not too much larger than the feasible solution, the computational cost of solving NLACR will be considerably less than that of solving NLAC due to the reduction in size of the number of integer solutions.

4.6 Computational results

In this section we compare the performance of our models to existing approaches. The resulting mixed integer linear and second-order cone programs were solved using the modeling language AMPL [54] and solver CPLEX [1] on a desktop computer representative of current standards. Objectives are given in terms of relative (unitless) values to facilitate comparison. Mixed integer semidefinite programs were enumeratively modeled in CVX [65] and solved with SeDuMi [117].

4.6.1 DC models

The main advantage in using LDC over DM is the retention of constraint (4.17) without the introduction a large number of binary variables. Of course, this constraint only has influence when $\overline{\eta}_{ij}$ is not too much larger than the optimal η_{ij}. We compare the models on the 46-bus, 79-line Brazilian system of [68,103] and the 24-bus, 41-line IEEE reliability test system [67,96], respectively shown in Figs. 4-1 and 4-2. In the original Brazilian system, line additions are unlimited, effectively nullifying constraint (4.17) and reducing LDC to the hybrid model of [107]. We modify the Brazil system so as to observe the differences in using LDC by setting $\overline{\eta}_{ij} = 2$ for all $(i,j) \in \Omega$.

We give the objective value and running time of DM and LDC, as well as the hybrid model of [107] in Table 4.1. In both cases, LDC achieves an objective between the hybrid model and DM, while requiring twice the time of the hybrid model and substantially less time than DM. In practical terms, LDC has similar efficiency to but greater accuracy than the hybrid model, and thus, like the hybrid model, can be applied to much larger problems than the disjunctive model.

Table 4.1: Efficiency of DC models

Model	DM		LDC		Hybrid	
	Obj.	Time	Obj.	Time	Obj.	Time
IEEE RTS	4.01	1.25	3.61	0.62	3.45	0.35
Brazilian	1.63	10.36	1.45	1.61	1.41	0.71

4.6.2 Linear AC models

We demonstrate LAC on two of the example systems from [106], which are AC versions of the Garver's six bus, fifteen-candidate line system [57], shown in Fig. 4-3 and the Brazilian test system of the previous section. Tables 4.2, and 4.3 show the objective value and solution reported for the nonlinear approach in [106] (NL) and obtained by the linear model LAC with $\tau^2 = 1$ and $\tau^2 = 0$ for all $(i,j) \in \Omega$. Problem data, including preexisting networks Ω_0, can be found in [106]. Running times in seconds are reported for each linear model as well. In the 'line additions' section of each table,

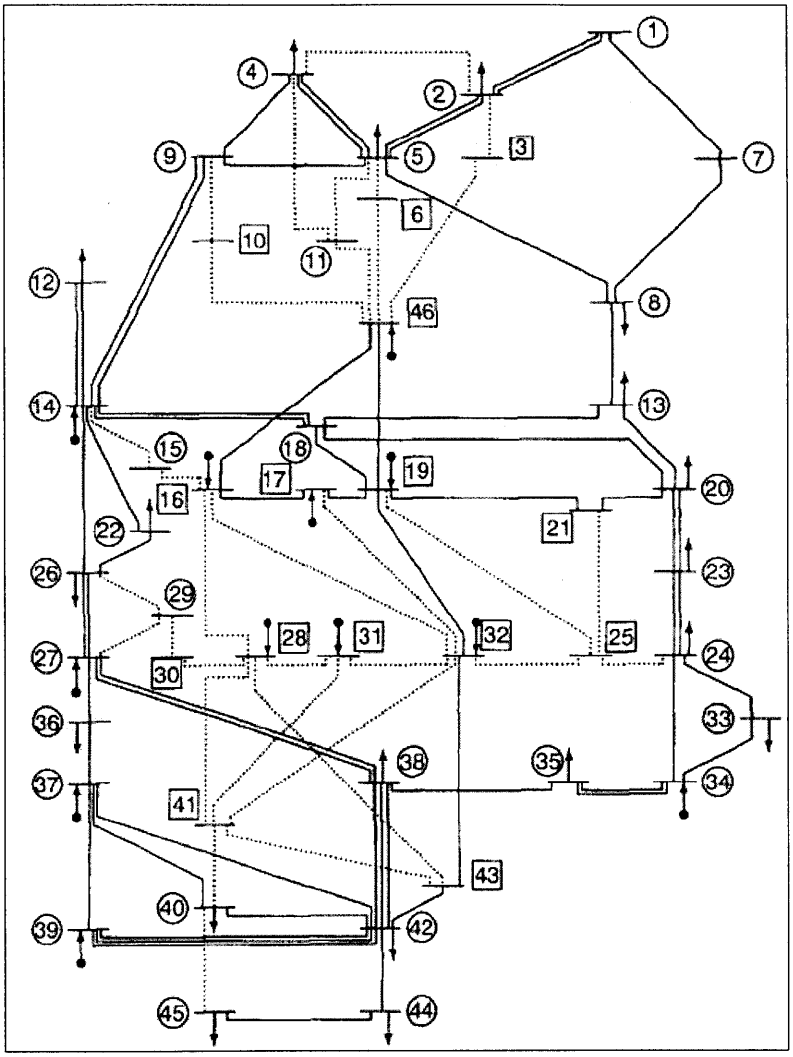

Figure 4-1: 46-bus Brazilian system (from [68]). Dashed lines represent candidate additions without existing lines, and solid lines existing lines (which are also candidates for additions).

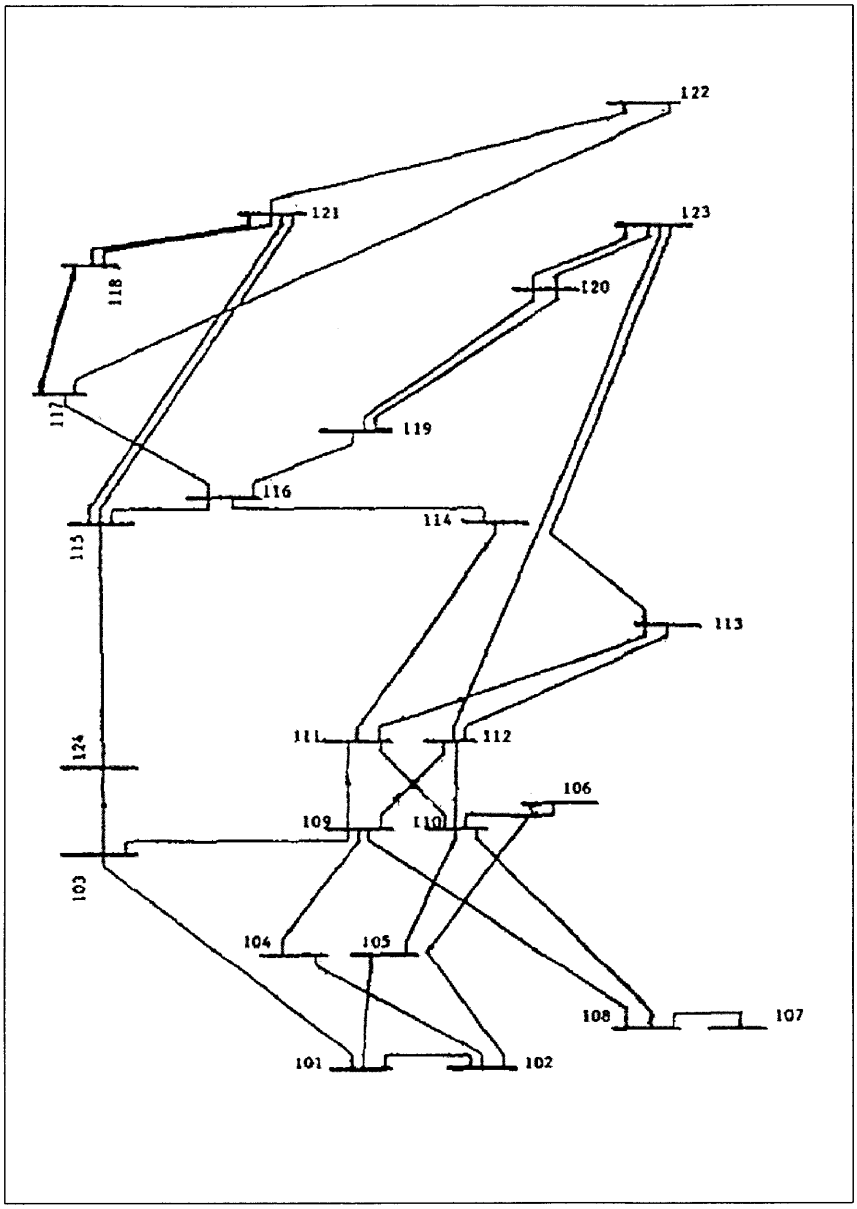

Figure 4-2: 24-bus IEEE reliability test system (from [96])

the left column indicates which line a given row corresponds to, and the other columns how many additions to that line were made by each algorithm; lines not listed were changed by none of the algorithms. LACB performed identically to LAC on these examples, and so is not shown. Note that we do not consider reactive power source allocation, and so our solutions for the latter two examples correspond to slightly different scenarios than those in [106]; we include the solutions for thoroughness.

Table 4.2: Garver's six bus system

Model	NL [106]	LAC, $\tau^2 = 1$	LAC, $\tau^2 = 0$
Obj.	260	190	160
Time	-	0.18	0.13
Line additions with no preexisting network			
1 - 5	1	1	0
2 - 3	1	2	0
2 - 6	3	1	2
3 - 5	2	2	2
4 - 6	3	2	2

Table 4.3: Brazilian system

Model	NL [106]	LAC, $\tau^2 = 1$	LAC, $\tau^2 = 0$
Obj.	10.258	10.800	8.254
Time	-	7.4	3.3
Line additions			
5 - 6	2	2	0
5 - 11	0	0	2
6 - 46	1	1	0
11 - 46	0	0	1
12 - 14	0	1	0
14 - 26	0	1	0
18 - 19	0	0	1
19 - 25	1	0	0
20 - 21	1	2	2
20 - 23	0	2	1
24 - 25	1	0	0
28 - 31	0	1	1
31 - 32	0	1	1
42 - 43	1	2	2
42 - 44	1	0	0

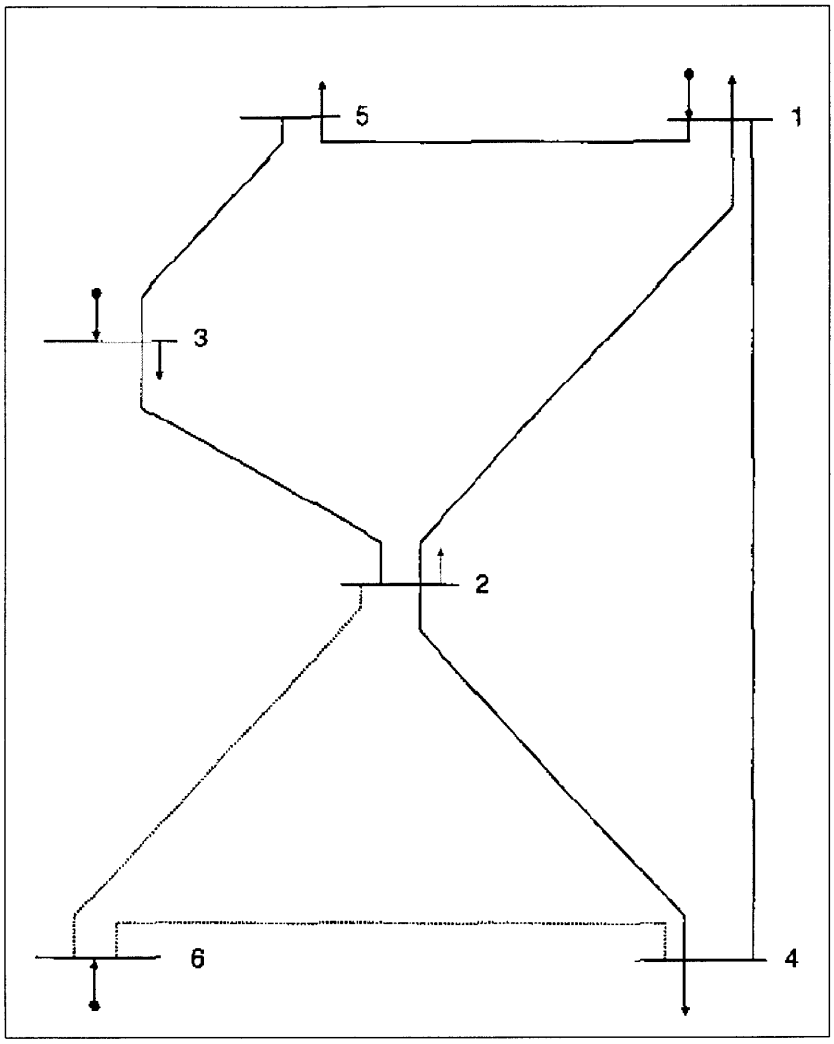

Figure 4-3: Candidate with existing networks (solid) and candidate without existing networks (dashed) in Garver's six bus system (from [107])

On the six bus system with $\Omega_0 = 0$ (Table 4.2), LAC with $\tau^2 = 1$ produces a feasible solution that has a lower objective than that reported in [106], highlighting its immediate applicability. With $\tau^2 = 0$ an infeasible, relaxed solution is found in less time. A number of other feasible solutions with objectives between 200 and 260 are easily found using the infeasible solution by simply enumerating over the set of single additions; we do not list them because none are superior to that found with $\tau^2 = 1$.

On the Brazilian system, both variants found solutions close to that given in [106]: by setting $\tau^2 = 1$, a more conservative solution is obtained, which can in fact have a higher objective than the nonlinear solutions, whereas setting $\tau^2 = 0$ yields relaxed solutions in considerably less time. Note that these results also confirm that a certain measure of discretion must be applied when interpreting relaxed solutions: some of the obtained solutions are likely to be infeasible, and would require reinforcement before being implementable. This point is revisited in later sections.

4.6.3 Nonlinear AC models

In this section we test SDAC and SOCAC on the six bus example of [106] with preexisting lines. Also included is LAC, with the following piecewise linear flow limits:

$$\begin{gathered} |p_{ij}| \leq \left(\eta_{ij} + \eta_{ij}^0\right) \overline{s}_{ij}, \qquad |q_{ij}| \leq \left(\eta_{ij} + \eta_{ij}^0\right) \overline{s}_{ij}, \\ |p_{ij}| + |q_{ij}| \leq \sqrt{2} \left(\eta_{ij} + \eta_{ij}^0\right) \overline{s}_{ij}. \end{gathered} \tag{4.93}$$

Tables 4.4 show the objective value and solution reported for the nonlinear approach in [106] (NL) and obtained by the linear (LAC), second-order cone (SOCAC), and semidefinite (SDAC) models. LAC and SOCAC each found solutions with the same objective; SOCAC, however, found three, whereas LAC found six, which indicates that SOCAC eliminated more low quality solutions than LAC. SDAC found three solutions with a higher objective than the other models. The bottom portion of Table 4.4 shows a single solution obtained by each model.

We note that the capacity constraint (4.38) is captured exactly in SOCAC and

Table 4.4: Garver's six bus system

Model	NL [106]	LAC	SOCAC	SDAC
No. solutions	-	6	3	3
Obj.	160	80	80	100
Line additions to a preexisting network				
2 - 6	2	2	2	1
3 - 5	2	1	1	2
4 - 6	2	0	0	1

SDAC, but can only be approximated within LAC. Thus, in this case, LAC corresponds to a looser nominal constraint set, putting it on slightly weaker footing than SOCAC and SDAC.

4.6.4 Shipboard power system

Shipboard systems have much shorter lines than terrestrial systems, and can have significant amounts of reactive power consumption, invalidating the assumptions of DC power flow and hence necessitating the use of an AC model. In this section we use LAC to optimize the a power system abstracted from a notional shipboard distribution system. Note that our intent is not to describe a specific design for the electric ship, but to solve an abstraction representative of its scale and heterogeneity, which can serve as a foundation for more detailed modeling.

Shipboard distribution system

We apply LAC to a 19-bus, 46-candidate line example which was abstracted from a notional shipboard power system [22]. Tables 4.5 and 4.6 contain all relevant problem data. Reactive power limits are assumed to be one tenth of real power limits (as in [106]), reactance and resistance are both set to length over line capacity, line costs to length times capacity, and $\overline{\eta}$ to two for all lines. The initial layout, η^0, encodes the power converter modules' (PCM) ring-bus arrangement. There are varying voltages levels throughout the ship, and so to maintain the simplicity of this example voltage limits are not enforced in this example. The flow limit approximation (4.93) was again used here.

The solution was obtained in 1.0 seconds on a standard laptop. Table 4.7 and Fig. 4-4 show which lines were selected (including the base design). Inspection shows that large loads are connected directly to large generators, as expected. Non-intuitive connections, or lack of connection elsewhere are generally due to the fact that the z-distances are not evident in the figure, and that certain connections were simply not part of the allowable set in Table 4.5.

Table 4.5: Line data

Line	Length (m)	s (MW)	η^0	Line	Length (m)	s (MW)	η^0
1 - 4	23.4	20.3	0	6 - 9	27.5	20.3	0
1 - 5	14.9	20.3	0	6 - 10	16.4	20.3	0
1 - 9	19.6	20.3	0	6 - 14	25.6	20.06	1
1 - 10	43.3	20.3	0	6 - 15	48.7	20.06	0
1 - 14	55.5	20.06	0	6 - 16	10.7	40	0
1 - 15	75.6	20.06	0	6 - 17	31.2	40	0
1 - 16	37.6	40	0	7 - 9	58.9	3.3	0
1 - 17	13.5	40	0	7 - 10	35	3.3	0
2 - 4	13.7	3.3	0	7 - 14	16.2	3.06	0
2 - 5	24.6	3.3	0	7 - 15	17.3	3.06	0
2 - 9	20.9	3.3	0	7 - 16	35.5	23	0
2 - 10	53	3.3	0	7 - 17	62.6	23	0
2 - 14	57.4	3.06	0	8 - 9	21	0.6	0
2 - 15	85.3	3.06	0	8 - 10	22.9	0.6	0
2 - 16	47.3	23	0	9 - 14	42.7	0.36	1
2 - 17	14.8	23	0	11 - 14	14.4	0.12	0
3 - 4	17	0.6	0	11 - 15	19.1	0.12	0
3 - 5	21.3	0.6	0	12 - 14	43.1	0.12	0
4 - 5	38.3	0.6	1	12 - 15	24.6	0.12	0
4 - 6	50.3	20.3	0	13 - 14	39.5	0.12	0
4 - 7	81.7	3.3	0	13 - 15	32.8	0.12	0
4 - 9	27.8	0.6	1	14 - 15	33.5	0.12	1
5 - 6	29.6	20.3	0	16 - 18	62.1	21.5	0
5 - 7	63.4	3.3	0	16 - 19	70.1	21.5	0
5 - 10	28.4	0.6	1	17 - 18	41.8	21.5	0
5 - 15	61.9	0.36	1	17 - 19	33.8	21.5	0

Multiple scenarios

We now give a brief example illustrating the application of Section 4.4.2 to the shipboard example, now with two sets of demands loosely representing turning left and

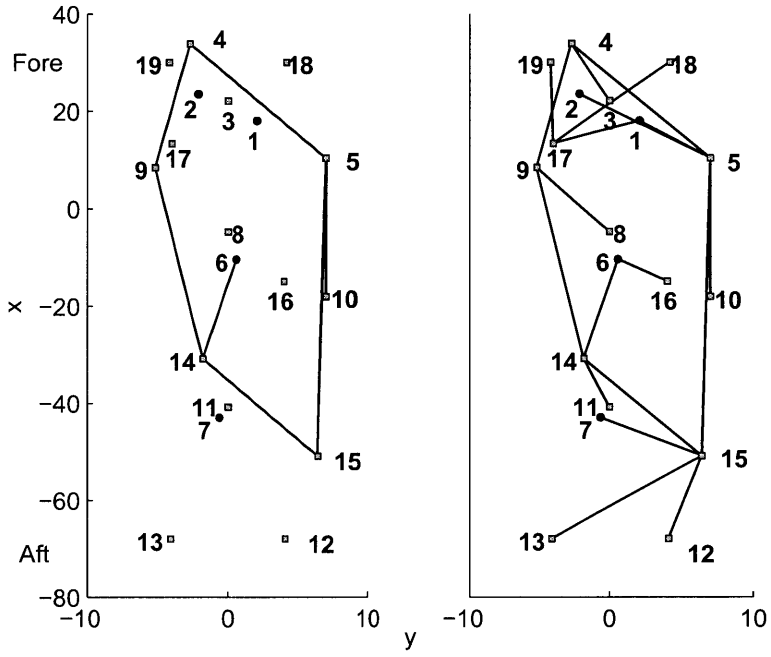

Figure 4-4: The existing network for the shipboard example, η^0, on the left, and the solution with existing network on the right. Buses are arranged geographically according to x and y coordinates given in Table 4.5 (the aspect ratio has been modified to aid viewing), with squares denoting loads and circles generation. Note that Buses 17 and 18 are not connected to Bus 3.

Table 4.6: Bus real power limits and locations

Bus	$\underline{p}$ (kW)	$\overline{p}$ (kW)	x (m)	y (m)	z (m)
1: fwd. mn. gen.	0	35000	18.0	2.1	5.8
2: fwd. aux. gen.	0	3500	23.5	-2.1	5.8
3: PCM 2a	-500	-500	22.1	0	5.6
4: PCM 1a	-500	-500	33.8	-2.7	3
5: PCM 1a	-500	-500	10.4	7.0	8.2
6: aft mn. gen.	0	35000	-10.4	0.6	5.8
7: aft aux. gen.	0	3500	-43.0	-0.6	5.8
8: PCM 2a	-500	-500	-4.7	0	5.6
9: PCM 1a	-500	-500	8.5	-5.2	3
10: PCM 1a	-500	-500	-18	7	8.2
11: PCM 2a	-100	-100	-40.8	0	5.6
12: port rud.	-50	-50	-68	4.1	3.0
13: stbd. rud.	-50	-50	-68	-4.1	3
14: PCM 1a	-100	-100	-30.8	-1.8	3
15: PCM 1a	-100	-100	-50.9	6.4	8.2
16: port motor	-37000	-37000	-14.9	4	3
17: stbd. motor	-37000	-37000	13.4	-4	3
18: port rdr.	-2300	-2300	30	4.2	20
19: stbd. rdr.	-2300	-2300	30	-4.2	20

Table 4.7: LAC solution

Line	Additions
1 - 5	1
1 - 17	1
2 - 5	1
3 - 4	2
6 - 16	1
7 - 15	1
8 - 9	1
9 - 14	2
11 - 14	1
12 - 15	1
13 - 15	1
17 - 18	1
17 - 19	1

right via asymmetric propulsion. The power specifications, which differ from the first example only in the last four buses, are given in kW in Table 4.8. The remaining parameters are determined as in the first shipboard example.

Table 4.9 show the solution given by LAC as adapted to the multiple scenario

Table 4.8: Bus real power limits for two scenarios

Bus	$\underline{p}_1$	$\overline{p}_1$	$\underline{p}_2$	$\overline{p}_2$
16: port motor	-37000	-37000	-1000	-1000
17: stbd. motor	-1000	-1000	-37000	-37000
18: port rdr.	0	0	-2300	-2300
19: stbd. rdr.	-2300	-2300	0	0

formulation MSAC. Table 4.9 and Fig. 4-5 show the solutions obtained for each individual scenario, the result of simply overlaying the separate solutions (taking the maximum of each solution over all lines), and lastly the solutions given by the multiple scenario formulation. Note that because no scenario fully utilizes generation capacity, the generator at bus seven is unused.

Table 4.9: LAC solution for two scenarios

Line	Scenario 1	Scenario 2	Overlayed	Together
1 - 5	0	1	1	1
1 - 17	0	1	1	1
2 - 17	1	0	1	0
2 - 4	0	1	1	1
3 - 4	1	1	1	1
6 - 16	1	1	2	1
7 - 10	1	0	1	0
8 - 9	0	1	1	1
8 - 10	1	0	1	0
11 - 14	2	2	2	2
11 - 15	2	2	2	2
12 - 15	1	1	1	1
13 - 14	1	1	1	1
14 - 15	1	1	1	1
17 - 18	0	1	1	1
17 - 19	1	0	1	1

4.6.5 Interpretation of results

In Section 4.5, the immediate next step to finding a relaxed solution is posed. We now discuss its tractability in light of this section's numerical examples. The performance of LAC on the six-bus system demonstrates the immediate gains from using a relaxation instead of a nonlinear approach at the outset: an objective of 110 is obtained

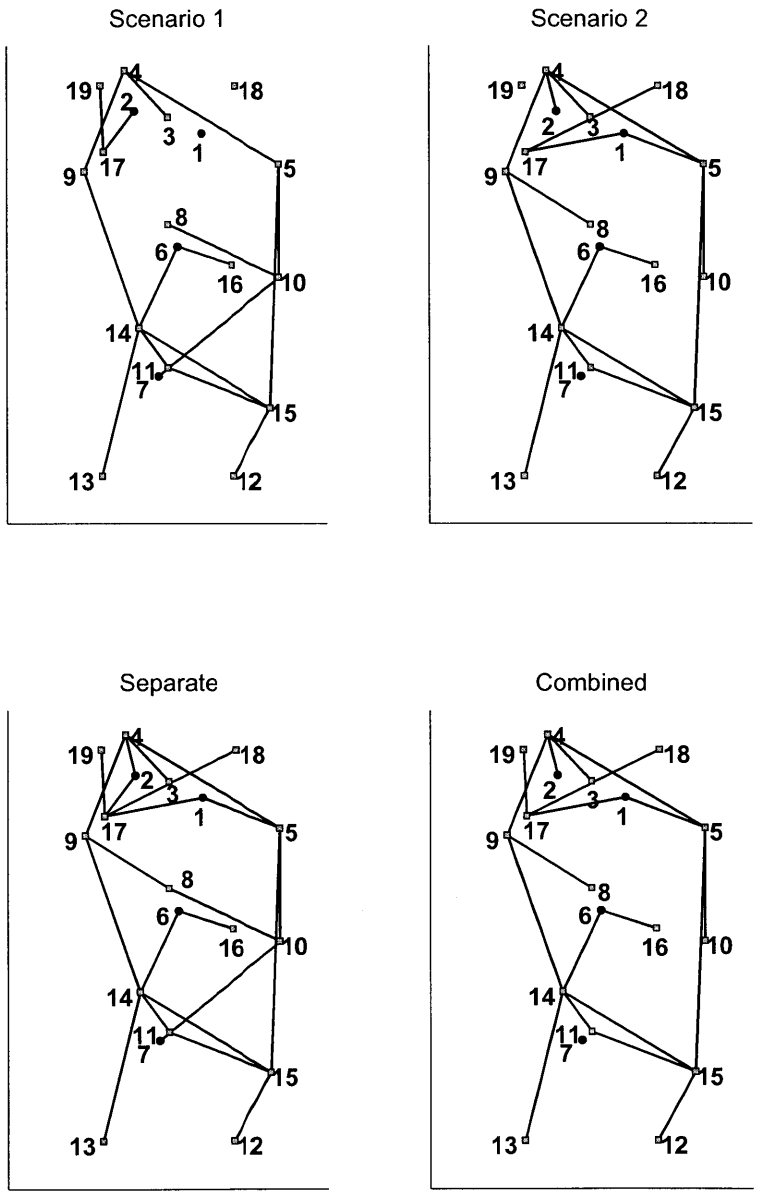

Figure 4-5: Layout for the shipboard system under two scenarios considered separately, overlayed, and together

by simply adding a single line to the solution in Table 4.2, a substantial improvement over the nonlinear heuristic's solution, which has an objective value of 160. The objective improvement further evidences the safeguard from bad local minima provided by using a relaxed solution as input data.

In the absence of an initial solution (relaxed or otherwise), NLACR represents the transmission system planning problem in full. The reinforcement of the relaxed solution is an application of NLACR, and illustrates the simplification enabled by relaxations: the addition could be identified by inspection, or could have easily been found through a brute force approach over a smaller number of discrete variables, reduced by the relaxed solution. In a larger problem, enumeration will likely still be too expensive, but we can similarly expect nonlinear branch and bound approaches to become more effective.

4.7 Summary

Using lift-and-project-based mixed-integer conic relaxations, we obtain mild improvements over existing linear DC models, and formulate the first conic AC models, which compare well with the more expensive nonlinear approach of [106]. As an alternative approach, the AC model substantially simplifies transmission system design by circumventing DC approximations.

There are multiple venues for future work in this context. One is the development of a general purpose software tool along the lines of the Gloptipoly [69] semidefinite relaxation suite, but which automatically generates linear relaxations of a specified order and calls linear rather than semidefinite solvers. Within power system design and operation there is an abundance of optimization problems complicated by low-order polynomial nonlinearities arising from electrical physics. The scale and often discrete nature of these problems calls for mixed integer linear and, pending further advancement, conic programming approaches. Complementary to the application of relaxations is the systematic development of procedures to augment relaxed solutions, e.g. for solving the nonconvex, mixed integer nonlinear program in Section

4.5. Clearly there are a plethora of approaches to such a problem, and it is unlikely that a single, comprehensively superior one exists for a large, NP-hard problem like transmission planning; yet, a strong pairing will strengthen the applicability of either approach by simultaneously addressing the infeasibility of relaxations and the scalability problems of basic formulations.

Chapter 5

Distribution system reconfiguration

5.1 Introduction

Distribution system reconfiguration entails choosing the combination of open and closed switches which optimizes certain performance criteria while maintaining a radial network topology [13, 29]. We develop new mixed integer quadratic (QP) [19], quadratically constrained (QCP), and second-order cone programming (SOCP) [93] formulations. The new formulations are accurate and easily solved to optimality using commercial software, enabling reconfiguration to be performed with higher or even real-time frequency. Such capability will be fundamental to minimizing losses and maintaining power quality modern distribution systems facing highly variable loads, e.g. from electric vehicles. A second application venue is the all-electric ship, for which quality of service, e.g. maintaining voltage levels, has been identified as a central objective [43]. The formulations, implicit in which are new load flow expressions for radial networks, extend beyond reconfiguration to many radial network optimization problems, such as sizing and location of capacitors [14] and distributed generation [27].

5.2 The *DistFlow* equations

We will make extensive use of the *DistFlow* equations for radial AC networks [13]. Let p_{ij} and q_{ij} denote the real and reactive powers at bus i going to j, v_i voltage magnitude, and p_i^L and q_i^L real and reactive loads at bus i. Let V be the set of buses, E be the set of lines, and r_{ij} and x_{ij} be line resistance and reactance. Unless otherwise specified, single-subscript constraints are over all i in V, and double-subscripted constraints are over all (i,j) in E. The *DistFlow* equations are given by

$$\sum_{k:(i,k)\in E} p_{ik} = p_{ji} - r_{ij}\frac{p_{ji}^2 + q_{ji}^2}{v_j^2} - p_i^L \tag{5.1}$$

$$\sum_{k:(i,k)\in E} q_{ik} = q_{ji} - x_{ij}\frac{p_{ji}^2 + q_{ji}^2}{v_j^2} - q_i^L \tag{5.2}$$

$$v_i^2 = v_j^2 - 2\left(r_{ij}p_{ji} + x_{ij}q_{ji}\right) + \left(r_{ij}^2 + x_{ij}^2\right)\frac{p_{ji}^2 + q_{ji}^2}{v_j^2} \tag{5.3}$$

5.3 Quadratic programming

In this section we use the *simplified DistFlow* equations [13], which are obtained by dropping all quadratic terms and (5.3). Let E^S be the subset of E with switches, V^F be the subset of V which are feeders, p_i^F and q_i^F, $i \in V^F$, be real and reactive powers from the feeders, and M be a sufficiently large disjunctive parameter. The following is a mixed integer QP for loss minimization [19].

$$\min_{p,q,y,z} \quad \sum_{(i,j)} r_{ij}\left(p_{ij}^2 + q_{ij}^2\right) \tag{5.4}$$

$$\text{s.t.} \quad \sum_{j:(i,j)\in E} p_{ji} - p_{ij} = p_i^L \qquad i \in V/V^F \tag{5.5}$$

$$\sum_{j:(i,j)\in E} q_{ji} - q_{ij} = q_i^L \qquad i \in V/V^F \tag{5.6}$$

$$\sum_{j:(i,j)\in E} p_{ij} = p_i^F \qquad i \in V^F \tag{5.7}$$

$$\sum_{j:(i,j)\in E} q_{ij} = q_i^F \qquad i \in V^F \tag{5.8}$$

$$0 \leq p_{ij} \leq M z_{ij} \tag{5.9}$$

$$0 \leq q_{ij} \leq M z_{ij} \tag{5.10}$$

$$z_{ij} \geq 0 \tag{5.11}$$

$$z_{if} = 0 \quad f \in V^F \tag{5.12}$$

$$z_{ij} + z_{ji} = 1 \quad (i,j) \in E \backslash E^S \tag{5.13}$$

$$z_{ij} + z_{ji} = y_{ij} \quad (i,j) \in E^S \tag{5.14}$$

$$\sum_{j:(i,j)\in E} z_{ji} = 1 \quad i \in V \backslash V^F \tag{5.15}$$

$$y_{ij} \in \{0,1\} \quad (i,j) \in E^S \tag{5.16}$$

The radiality constraints are similar to those of [26] and [81]. Two variables z_{ij} and z_{ji} are associated with each line designating which direction, if any, flow may travel. With each switched line is associated a single binary variable y_{ij}, which is zero if the switch is open and one if closed. We must now show that this scheme always results in a radial configuration.

Lemma 3. *Any feasible z must be zeros and ones, and for each feeder it describes the edges of an unweighted, directed tree graph with a root node (arborescence).*

Proof. Assume y is fixed, and let $E^y = \{(i,j) \in E^S : y_{ij} = 1\} \cup E \backslash E^S$. Consider a path through E^y beginning at a feeder, which we label bus zero. For any $(0,i) \in E^y$, $z_{0i} = 1$, and, by (5.15), $z_{ij} = 1$ for any $j \in V \backslash \{0\}$; we see by induction along the path that any z on a path from the feeder must be oriented such that it is zero going 'in' and one 'out', and therefore no two paths originating at a feeder can meet (forming a loop if they are from the same feeder). If a loop is formed which does not contain a feeder, its buses are not receiving any flow, and (5.5) and (5.6) cannot be satisfied. We conclude that z must describe an arborescence for each feeder; to do so, E^y must itself be composed of trees, and hence any feasible y results in a radial configuration. □

5.4 Quadratically constrained programming

If we extend our framework to QCP, we enhance our modeling capability in three ways. First, line flow limits can be expressed $p_{ij}^2 + q_{ij}^2 \leq S_{ij}^2$, where S denotes line capacity; these are new constraints. Second, recognizing that the equalities in (5.5) and (5.6) are identical to requiring that the flow into a bus be greater than the load plus the outgoing flow, losses may be approximated within flow conservation by replacing (5.5) and (5.6) with

$$\sum_{j:(i,j)\in E} p_{ji} - p_{ij} - r_{ij}\left(p_{ji}^2 + q_{ji}^2\right) \geq p_i^L \tag{5.17}$$

$$\sum_{j:(i,j)\in E} q_{ji} - q_{ij} - x_{ij}\left(p_{ji}^2 + q_{ji}^2\right) \geq q_i^L \tag{5.18}$$

Then, with losses accounted for in flow conservation, the sum of the feeder flows $\sum_{i\in V^F} p_i^F$ may be equivalently (and more efficiently) used as a loss reduction objective. Third, the load balancing formulation of [29] is accommodated by adding the constraint $p_{ij}^2 + q_{ij}^2 \leq S_{ij}^2 t$ and minimizing the objective t.

5.5 Second-order cone programming

SOCP [93] is a polynomial-time generalization of convex QCP. Its mixed integer counterpart is an active area of research [46, 120], and is currently handled by some commercial solvers. We derive an SOCP approximation of the *DistFlow* equations in which only the last term in (5.3) is dropped. The approximation is obtained by replacing (5.17) and (5.18) with the following constraints:

$$\tilde{p}_i = -p_i^L + \sum_{j:(i,j)\in E} p_{ji} - p_{ij} \tag{5.19}$$

$$\tilde{q}_i = -q_i^L + \sum_{j:(i,j)\in E} q_{ji} - q_{ij} \tag{5.20}$$

$$\tilde{v}_i^2 \leq v_j^2 + M\left(1 - z_{ji}\right) \tag{5.21}$$

$$\tilde{v}_i^2 \geq v_j^2 - M\left(1 - z_{ji}\right) \tag{5.22}$$

$$r_{ij}\left(p_{ji}^2+q_{ji}^2\right)\leq \tilde{v}_i^2\tilde{p}_i \tag{5.23}$$

$$x_{ij}\left(p_{ji}^2+q_{ji}^2\right)\leq \tilde{v}_i^2\tilde{q}_i \tag{5.24}$$

$$v_i^2\leq v_j^2-2\left(r_{ij}p_{ji}+x_{ij}q_{ji}\right)+M\left(1-z_{ji}\right) \tag{5.25}$$

$$v_i^2\geq v_j^2-2\left(r_{ij}p_{ji}+x_{ij}q_{ji}\right)-M\left(1-z_{ji}\right) \tag{5.26}$$

$$v_i^2=1\text{ pu}\qquad i\in V^F \tag{5.27}$$

We are again using disjunctive constraints in (5.21), (5.22), (5.25), and (5.26), which are only 'active' when $z_{ji}=1$. The purpose of the extra variables $\tilde{p}_i$ and $\tilde{q}_i$ is to put the constraints into an SOCP form recognizable by commercial solvers. Note that for a fixed network, these constraints constitute a new radial power flow approximation.

5.6 Computational examples

In this section we use each model to reconfigure the 32-bus test system of [13] shown in Fig. 5-1 and the 70-bus test system of [39] for the loss minimization and load balancing objectives as given in sections 5.3 and 5.4, and maximizing minimum voltage, which is accommodated linearly by maximizing t subject to $t\leq v_i^2$ for all i. For load balancing, the p.u. capacity of each line was somewhat arbitrarily assumed to be the reciprocal of its impedance's magnitude. We note that minimum voltage maximization with the *simplified DistFlow* equations is actually a linear program. The resulting mixed integer programs were solved using the modeling language AMPL [54] and solver CPLEX [1] on a desktop computer representative of current standards. Tables 5.1 and 5.2 give per unit objectives, load flow values computed for the corresponding configuration, and computation times for each model.

Each model found the optimal loss-minimizing switch configuration [81], which was determined to be optimal by enumeration in [63]. The QCP and SOCP models each found the same load balancing solution, with open switches (8,21), (9,10), (14,15), (28,29), and (31,32). As stated earlier, this load balancing formulation cannot be modeled within QP. The QP and SOCP models each found the same maximum minimum voltage, with switches (7,8), (9,10), (14,15), (28,29), and (32,33) open.

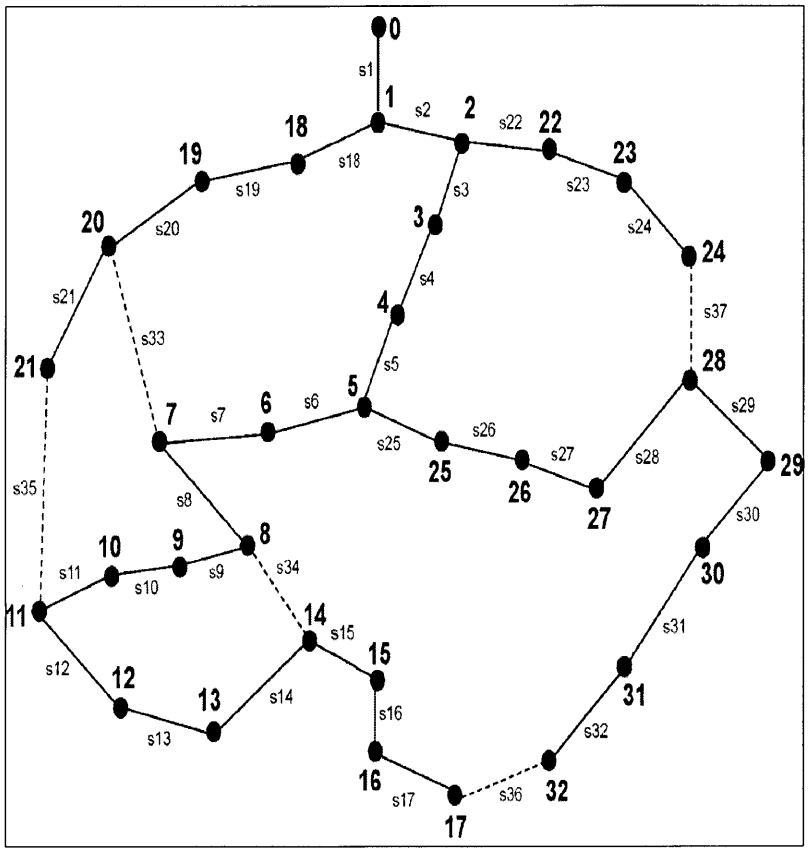

Figure 5-1: 32-bus test system (image from [81]). Solid and dashed lines respectively indicate open and closed switches in the nominal configuration.

Table 5.1: Optimization objectives, load flow values, and computation times for the 32-bus test system of [13]

Model	QP	QCP	SOCP
Loss minimization			
Objective	0.01273	0.01343	0.01404
Load flow	0.01395	0.01395	0.01395
Time (s)	0.30	1.43	12.80
Load balancing			
Objective	-	0.04134	0.04169
Load flow	-	0.04146	0.04146
Time (s)	-	2.31	18.06
Minimum voltage maximization			
Objective	0.94253	0.94107	0.94082
Load flow	0.9412871	0.9412865	0.9412871
Time (s)	2.09	7.34	18.67

The QCP model found a very slightly worse solution with (9,10) open instead of (10,11).

The second, larger example shown in Fig. 5-2, on which no particular approach exhibited better accuracy, is included to demonstrate the scaling of each approaches computation time. Objectives and load flow values are shown in Table 5.2, and Tables 5.3, 5.4, and 5.5 contain corresponding optimal configurations. Only switches that are open in at least one solution shown, with open switches denoted 0 and closed 1. The SOCP model is too slow for a system this size; clearly new algorithms must be developed before it is pragmatic. The QP model retains much of its efficiency, particularly for loss minimization, for which it required under a second. The QCP model again took times between the QP and SOCP models.

Lastly, we comment on the disparity between computation times across objectives: it must be recalled that these formulations are all NP-hard, and while some of the solvers employed are mature technologies, it is impossible to guarantee an efficient route to a solution. That said, the times obtained by the QP model are attractive, and suggest real-time applicability. Furthermore, they are an order of magnitude faster than times reported for recent heuristics: in [51], a genetic algorithm required 7.2 seconds on the 32-bus test system and 160 seconds on the 70-bus test system to

minimize losses. Table 5.6 provides computation times for various approaches tested in [63] on the 33-bus system, as well as that of [81]: no other method both finds the optimum and is faster than QP.

Table 5.2: Optimization objectives, load flow values, and computation times for the 70-bus test system of [39]

Model	QP	QCP	SOCP
Loss minimization			
Objective	0.02640	0.02852	0.03031
Load flow	0.03016	0.03018	0.03016
Time (s)	0.92	10.10	11310.48
Load balancing			
Objective	-	0.4394	0.4428
Load flow	-	0.44126	0.44132
Time (s)	-	226.24	1306.94
Minimum voltage maximization			
Objective	0.9223	0.9191	0.9186
Load flow	0.9247	0.9199	0.9199
Time (s)	40.59	737.10	4738.44

Table 5.3: Loss minimization solutions for the 70-bus test system of [39]. Only switches that are open in at least one solution shown, with open switches denoted 0 and closed 1.

Line	QP	QCP	SOCP
9 - 15	0	0	0
21 - 27	0	0	0
28 - 29	0	0	0
37 - 38	0	1	0
40 - 44	0	0	0
43 - 38	1	0	1
49 - 50	0	0	0
62 - 65	0	0	0
67 - 15	0	0	0

As a final examination of scaling, we evaluate the computation time of QP as a function of the number of lines, where each line is a switch. Each data point corresponds to a randomly generated network with between ten and ninety buses, separated by increments of ten. Resistances and reactances are drawn from uniform random variables between zero and one, and real and reactive loads from uniform

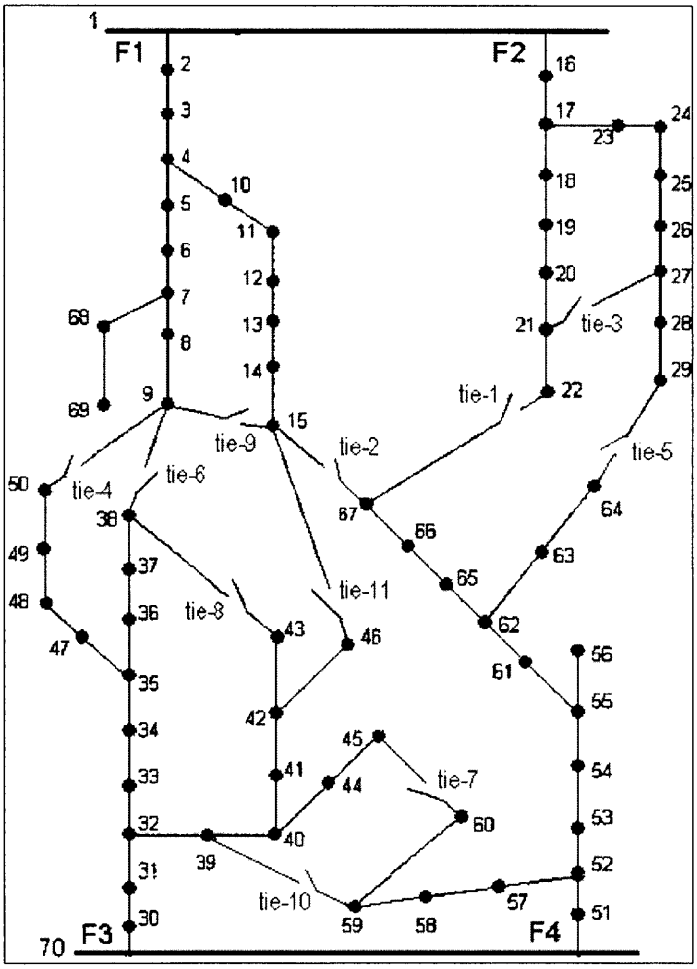

Figure 5-2: 70 bus test system in nominal tree configuration (image from [38]).

Table 5.4: Load balancing solutions for the 70-bus test system of [39]

Line	QCP	SOCP
8 - 9	1	0
14 - 15	0	1
21 - 27	0	0
27 - 28	0	1
29 - 64	1	0
42 - 43	1	0
43 - 38	0	1
45 - 60	0	0
48 - 49	0	0
62 - 65	0	1
65 - 66	1	0
67 - 15	0	0

Table 5.5: Voltage maximization solutions for the 70-bus test system of [39]

Line	QP	QCP	SOCP
9 - 15	0	0	0
21 - 27	0	0	0
28 - 29	0	0	0
36 - 37	1	1	0
37 - 38	0	1	1
43 - 38	1	0	1
49 - 50	0	0	0
58 - 59	0	1	1
59 - 60	1	0	0
62 - 65	0	0	0
67 - 15	0	0	0

random variables between zero and one-hundred. Twenty trials were performed for each number of buses. Fig. 5-3 shows the increase in time with number of discrete variables; as one would expect of an NP-hard problem, the increase in computation time is severe.

5.7 Summary

We have introduced three new convex, mixed integer programming models for distribution system reconfiguration. On an example, the QP model is by far the most efficient, yet also obtains good solutions, evidencing its practicality for very large

Table 5.6: Comparison of computation times (s) from a 2006 comparative study of reconfiguration algorithms for loss minimization on the 32-bus test system [63].

Algorithm	time (s)	Optimal?
[51]	7.2	yes
[81]	0.11	no
[41]	1.99	yes
[64]	0.87	yes
[113]	0.14	no
[62]	1.66	yes
[63]	0.96	no
QP	0.30	yes

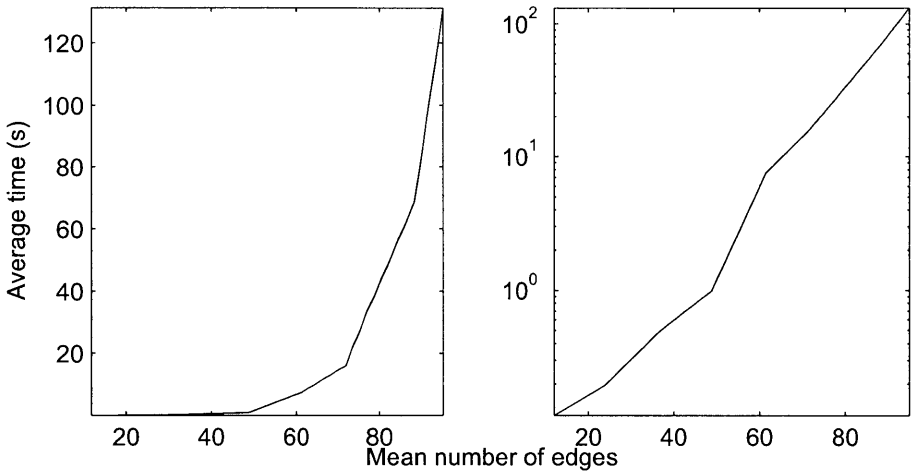

Figure 5-3: Average computation time versus average number of switches for loss minimization of randomly generated distribution networks, shown on normal (left) and logarithmic (right) y-axes

systems. The SOCP model appears to be more reliable in producing good solutions, but rather expensive computationally; it is however reasonable to expect substantial improvements in mixed integer SOCP algorithms in the near future, in which case the SOCP model will become a more scalable option.

Chapter 6

Conclusion

In this thesis, two older problems in power systems and a new problem in spectral graph theory have been addressed. We now conclude by identifying some future directions and broader connections with modern power systems, starting with the latter.

The sparsest cut has been the subject of much recent theoretical investigation, primarily concerning semidefinite programming relaxations coupled with rounding procedures. The new quantity q introduced in Section 3.3 generalizes the sparsest cut, and thus invites new analysis both of situations unmodeled by the sparsest cut, and of previously studied cases via the connection between spectral graph theory, a semidefinite programming perspective, and flow networks. Significant gains may be possible via a better embedding of network nodes. The eigenvalue μ^r in Section 3.3 maps flow network nodes to the real line. In contrast, recent successful relaxations of the sparsest cut embed graph vertices in the sphere, and therefore one might expect that there exists a superior relaxation of q which embeds network nodes in a sphere; however, such an approach would sacrifice eigenvalue specific perspectives. We note that because sparsest cut relaxations can be derived by lift-and-project procedures, their corresponding bounds may inform more general analyses, which include other lift-and-project relaxations such as those in Chapter 4.

Despite their respective problem statements having existed in distilled mathematical formats for many years, the results of Chapters 4 and 5 broadly inform other

problems in power systems via the accuracy and efficiency with which convex conic constraints can approximate steady state AC power flow. These expressions appear ubiquitously in both static and dynamic power system problems, and it is the author's opinion that for many such problems, there are conic optimizations by which they are well represented, and which can be reached either by a lift-and-project procedure or physics-based approximations. Thus there are many venues for future research within this theme, a few of which we name here:

- *Component placement:* Placement of components such as capcitors [14] and FACTS devices [58] is determined by their effect on power flows, and hence optimization must contain AC power flow constraints. Incorporation of convex conic formulations will allow optimization of component placement over much larger system sizes, rather then smaller, separate parts.

- *Market pricing:* All economic models are based on the DC power flow approximation [125], which neglects reactive power, loss, and voltage. A more detailed, conic formulation of optimal AC power flow can include information about losses and voltage and retain strong duality, yielding new 'price' quantities from multipliers associated with loss and voltage constraints.

- *Dynamic optimization and control:* Many new problems in power are inherently dynamic, for example storage, a primary use of which is buffering the grid from unpredictable spikes in renewable outputs. A discretized dynamic optimization problem must have AC power flow constraints at each stage. The dynamic problem, whether via a dynamic programming or Pontryagin based approach, will hence inherit the convexity of each stage, making the larger problem more tractable.

This is of course an incomplete list, but serves to demonstrate that AC power flow is foundational to nearly all power system problems, many of which can and should be formulated as optimizations. By expressing these problems as conic programs, the tractability of numerous problems in power systems is greatly enhanced.

Bibliography

[1] IBM ILOG CPLEX.

[2] IEEE 118 bus test system, power systems test case archive.

[3] U.S. Energy Information Administration. *Annual Energy Review 2009.* Department of Energy, 2010.

[4] R. K. Ahuja, T. L. Magnanti, and J. B. Orlin. *Network flows: theory, algorithms, and applications.* Prentice-Hall, Inc., Upper Saddle River, NJ, USA, 1993.

[5] N. Alguacil, A.L. Motto, and A.J. Conejo. Transmission expansion planning: a mixed-integer LP approach. *Power Systems, IEEE Transactions on*, 18(3):1070 – 1077, Aug. 2003.

[6] F. Alizadeh and D. Goldfarb. Second-order cone programming. *Mathematical Programming*, 95:3–51, 2003. 10.1007/s10107-002-0339-5.

[7] Farid Alizadeh. Interior point methods in semidefinite programming with applications to combinatorial optimization. *SIAM Journal on Optimization*, 5:13–51, 1993.

[8] G. Andersson, P. Donalek, R. Farmer, N. Hatziargyriou, I. Kamwa, P. Kundur, N. Martins, J. Paserba, P. Pourbeik, J. Sanchez-Gasca, R. Schulz, A. Stankovic, C. Taylor, and V. Vittal. Causes of the 2003 major grid blackouts in North America and Europe, and recommended means to improve system dynamic per-

formance. *Power Systems, IEEE Transactions on*, 20(4):1922–1928, November 2005.

[9] S. Arora, J. R. Lee, and A. Naor. Euclidean distortion and the sparsest cut. *J. Amer. Math. Soc.*, 21(1):1–21, 2008.

[10] S. Arora, S. Rao, and U. Vazirani. Expander flows, geometric embeddings and graph partitioning. *J. ACM*, 56:5:1–5:37, April 2009.

[11] Jos Arrillaga. *High voltage direct current transmission.* The institute of electrical engineers, London, UK, second edition, 1998.

[12] M.E. Baran and N.R. Mahajan. DC distribution for industrial systems: opportunities and challenges. *Industry Applications, IEEE Transactions on*, 39(6):1596 – 1601, 2003.

[13] M.E. Baran and F.F. Wu. Network reconfiguration in distribution systems for loss reduction and load balancing. *Power Delivery, IEEE Transactions on*, 4(2):1401 –1407, April 1989.

[14] M.E. Baran and F.F. Wu. Optimal capacitor placement on radial distribution systems. *Power Delivery, IEEE Transactions on*, 4(1):725 –734, January 1989.

[15] Richard Bellman. *Dynamic Programming.* Dover Publications, March 2003.

[16] A. Ben-Tal and A. Nemirovski. Robust truss topology design via semidefinite programming. *SIAM J. on Optimization*, 7:991–1016, April 1997.

[17] Aharon Ben-Tal and Arkadi Nemirovski. Robust optimization - methodology and applications. *Mathematical Programming*, 92(3):453–480, May 2002.

[18] Dimitri P. Bertsekas. *Nonlinear Programming.* Athena Scientific, 2004.

[19] Daniel Bienstock. Computational study of a family of mixed-integer quadratic programming problems. *Mathematical Programming*, 74:121–140, 1996.

[20] Roy Billinton and Ronald N. Allan. *Reliability evaluation of power systems.* Springer, second edition, 1996.

[21] S. Binato, M.V.F. Pereira, and S. Granville. A new Benders decomposition approach to solve power transmission network design problems. *Power Systems, IEEE Transactions on*, 16(2):235–240, May 2001.

[22] BMT Syntek. IPS electric plant one-line diagram for a notional destroyer, 2003.

[23] Otakar Boruvka. O jistm problmu minimlnm (about a certain minimal problem). *Prce mor. prrodoved. spol. v Brne III*, 3:37–58, 1926.

[24] Otakar Boruvka. Prspevek k reen otzky ekonomick stavby elektrovodnch st (contribution to the solution of a problem of economical construction of electrical networks). *Elektronick Obzor*, 15:153–154, 1926.

[25] S. Boyd and L. Vandenberghe. *Convex Optimization.* Cambridge University Press, New York, NY, USA, 2004.

[26] K.L. Butler, N.D.R. Sarma, and V. Ragendra Prasad. Network reconfiguration for service restoration in shipboard power distribution systems. *Power Systems, IEEE Transactions on*, 16(4):653–661, Nov 2001.

[27] G. Celli and F. Pilo. Optimal distributed generation allocation in mv distribution networks. In *Power Industry Computer Applications, 2001. PICA 2001. Innovative Computing for Power - Electric Energy Meets the Market. 22nd IEEE Power Engineering Society International Conference on*, 2001.

[28] J. Cheeger. A lower bound for the smallest eigenvalue of the Laplacian. *Problems in Analysis*, 1970.

[29] H.-D. Chiang and R. Jean-Jumeau. Optimal network reconfigurations in distribution systems: I: A new formulation and a solution methodology. *Power Delivery, IEEE Transactions on*, 5(4):1902–1909, Oct. 1990.

[30] H.-D. Chiang and R. Jean-Jumeau. Optimal network reconfigurations in distribution systems: II: Solution algorithms and numerical results. *Power Delivery, IEEE Transactions on*, 5(3):1568–1574, Jul. 1990.

[31] J. Choi, T. Tran, A.A. El-Keib, R. Thomas, H. Oh, and R. Billinton. A method for transmission system expansion planning considering probabilistic reliability criteria. *Power Systems, IEEE Transactions on*, 20(3):1606–1615, Aug. 2005.

[32] Moody T. Chu and Gene H. Golub. *Inverse Eigenvalue Problems: Theory, Algorithms, and Applications.* Oxford University Press, USA, 2005.

[33] F. R. K. Chung. *Spectral Graph Theory (CBMS Regional Conference Series in Mathematics, No. 92).* American Mathematical Society, February 1997.

[34] F. R. K. Chung. Laplacians and the Cheeger inequality for directed graphs. *Annals of Combinatorics*, 9:1–19, 2005.

[35] J.G. Ciezki and R.W. Ashton. Selection and stability issues associated with a navy shipboard DC zonal electric distribution system. *Power Delivery, IEEE Transactions on*, 15(2):665 –669, Apr 2000.

[36] S. Civanlar, J.J. Grainger, H. Yin, and S.S.H. Lee. Distribution feeder reconfiguration for loss reduction. *Power Delivery, IEEE Transactions on*, 3(3):1217 –1223, Jul. 1988.

[37] George B. Dantzig. *Linear Programming and Extensions.* Princeton University Press, 1998.

[38] D. Das. A fuzzy multiobjective approach for network reconfiguration of distribution systems. *Power Delivery, IEEE Transactions on*, 21(1):202 – 209, 2006.

[39] D. Das. Reconfiguration of distribution system using fuzzy multi-objective approach. *International Journal of Electrical Power and Energy Systems*, 28(5):331 – 338, 2006.

[40] T.E. DcDermott, I. Drezga, and R.P. Broadwater. A heuristic nonlinear constructive method for distribution system reconfiguration. *Power Systems, IEEE Transactions on*, 14(2):478 – 483, May 1999.

[41] T.E. DcDermott, I. Drezga, and R.P. Broadwater. A heuristic nonlinear constructive method for distribution system reconfiguration. *Power Systems, IEEE Transactions on*, 14(2):478 –483, may 1999.

[42] P. Diaconis and D. Stroock. Geometric bounds for eigenvalues of Markov chains. *The Annals of Applied Probability*, 1(1):36–61, 1991.

[43] N. Doerry and J. Amy. Implementing quality of service in shipboard power system design. In *IEEE Electric Ship Technologies Symposium*, pages 1–8, Apr. 2011.

[44] Norbert Doerry, Henry Robey, John Amy, and Chester Petry. Powering the future with the integrated power system. *Naval Engineers Journal*, 108(3):267–282, 1996.

[45] H.W. Dommel and W.F. Tinney. Optimal power flow solutions. *Power Apparatus and Systems, IEEE Transactions on*, PAS-87(10):1866 –1876, Oct. 1968.

[46] S. Drewes. *Mixed Integer Second Order Cone Programming.* PhD thesis, Technischen Universität Darmstadt, 2009.

[47] Zivi E. and McCoy T.J. Control of a shipboard integrated power system. In *Proceedings of the 33th Annual Conference on Information Sciences and Systems*, March 1999.

[48] Alan Edelman. *Eigenvalues and condition numbers of random matrices.* PhD thesis, 1989.

[49] W. El-Khattam, K. Bhattacharya, Y. Hegazy, and M.M.A. Salama. Optimal investment planning for distributed generation in a competitive electricity market. *Power Systems, IEEE Transactions on*, 19(3):1674–1684, Aug. 2004.

[50] P. Elias, A. Feinstein, and C. Shannon. A note on the maximum flow through a network. *Information Theory, IRE Transactions on*, 2(4):117–119, December 1956.

[51] B. Enacheanu, B. Raison, R. Caire, O. Devaux, W. Bienia, and N. HadjSaid. Radial network reconfiguration using genetic algorithm based on the matroid theory. *Power Systems, IEEE Transactions on*, 23(1):186 –195, Feb. 2008.

[52] P. Erdős and A. Rényi. On random graphs. I. *Publ. Math. Debrecen*, 6:290–297, 1959.

[53] M. Fiedler. Algebraic connectivity of graphs. *Czechoslovak Mathematical Journal*, 23(98):298–305, 1973.

[54] Robert Fourer, David M. Gay, and Brian W. Kernighan. *AMPL: A Modeling Language for Mathematical Programming.* Duxbury Press, November 2002.

[55] S. Friedland. On inverse multiplicative eigenvalue problems for matrices. *Linear Algebra and its Applications*, 12(2):127 – 137, 1975.

[56] D. Gale. A theorem on flows in networks. *Pacific Journal of Mathematics*, 7(2):1073–1082, 1957.

[57] L.L. Garver. Transmission network estimation using linear programming. *Power Apparatus and Systems, IEEE Transactions on*, PAS-89(7):1688–1697, Sept. 1970.

[58] S. Gerbex, R. Cherkaoui, and A.J. Germond. Optimal location of multi-type facts devices in a power system by means of genetic algorithms. *Power Systems, IEEE Transactions on*, 16(3):537 –544, aug 2001.

[59] M. X. Goemans. Semidefinite programming in combinatorial optimization. *Mathematical Programming*, 79:143–161, 1997.

[60] M. X. Goemans and D. P. Williamson. Improved approximation algorithms for maximum cut and satisfiability problems using semidefinite programming. *J. ACM*, 42:1115–1145, November 1995.

[61] G. H. Golub and C. F. Van Loan. *Matrix computations*. Johns Hopkins University Press, Baltimore, MD, USA, 3rd edition, 1996.

[62] F.V. Gomes, Jr. Carneiro, S., J.L.R. Pereira, M.P. Vinagre, P.A.N. Garcia, and L.R. Araujo. A new heuristic reconfiguration algorithm for large distribution systems. *Power Systems, IEEE Transactions on*, 20(3):1373 – 1378, aug. 2005.

[63] F.V. Gomes, S. Carneiro, J.L.R. Pereira, M.P. Vinagre, P.A.N. Garcia, and Leandro Ramos de Araujo. A new distribution system reconfiguration approach using optimum power flow and sensitivity analysis for loss reduction. *Power Systems, IEEE Transactions on*, 21(4):1616 –1623, nov. 2006.

[64] S.K. Goswami and S.K. Basu. A new algorithm for the reconfiguration of distribution feeders for loss minimization. *Power Delivery, IEEE Transactions on*, 7(3):1484 –1491, jul 1992.

[65] Michael Grant, Stephen Boyd, and Yinyu Ye. CVX: Matlab Software for Disciplined Convex Programming, August 2008.

[66] S. Granville and M. V. F. Pereira. Analysis of the linearized power flow model in Bender's decomposition. Technical report, Stanford, CA, USA, 1985. EPRI-report RP 2473-6.

[67] C. Grigg, P. Wong, P. Albrecht, R. Allan, M. Bhavaraju, R. Billinton, Q. Chen, C. Fong, S. Haddad, S. Kuruganty, W. Li, R. Mukerji, D. Patton, N. Rau, D. Reppen, A. Schneider, M. Shahidehpour, and C. Singh. The IEEE reliability test system-1996. *Power Systems, IEEE Transactions on*, 14(3):1010 –1020, Aug. 1999.

[68] S. Haffner, A. Monticelli, A. Garcia, J. Mantovani, and R. Romero. Branch and bound algorithm for transmission system expansion planning using a trans-

portation model. *IEE Proceedings - Generation, Transmission and Distribution*, 147(3):149–156, 2000.

[69] Didier Henrion and Jean Bernard Lasserre. Gloptipoly: Global optimization over polynomials with Matlab and SeDuMi. *ACM Trans. Math. Softw.*, 29(2):165–194, 2003.

[70] A. Hoffman. Some recent applications of the theory of linear inequalities to extremal combinatorial analysis. In *Proc. Symp. in Applied Mathematics, Amer. Math. Soc.*, pages 113–127, 1960.

[71] R. A. Horn and C. R. Johnson. *Matrix Analysis.* Cambridge University Press, 1990.

[72] T. C. Hu. Multi-commodity network flows. *Operations Research*, 11(3):344–360, 1963.

[73] Y. Ito, Y. Zhongqing, and H. Akagi. DC microgrid based distribution power generation system. In *Power Electronics and Motion Control Conference, 2004. IPEMC 2004. The 4th International*, volume 3, pages 1740–1745 Vol.3, 2004.

[74] J. Jonnes. *Empires of light: Edison, Tesla, Westinghouse, and the race to electrify the world.* Random House, 2004.

[75] L. R. Ford Jr. and D. R. Fulkerson. Maximal flow through a network. *Canadian Journal of Mathematics*, 8:399–404, 1956.

[76] L. R. Ford Jr. and D. R. Fulkerson. *Flows in Networks.* Princeton University Press, 1962.

[77] P. Kall and S. W. Wallace. *Stochastic programming.* John Wiley & Sons, Chichester, 1994.

[78] N. Karmarkar. A new polynomial-time algorithm for linear programming. In *Proceedings of the sixteenth annual ACM symposium on Theory of computing*, STOC '84, pages 302–311, New York, NY, USA, 1984. ACM.

[79] F. Katiraei, M.R. Iravani, and P.W. Lehn. Micro-grid autonomous operation during and subsequent to islanding process. *Power Delivery, IEEE Transactions on*, 20(1):248–257, Jan. 2005.

[80] S.A. Kazarlis, A.G. Bakirtzis, and V. Petridis. A genetic algorithm solution to the unit commitment problem. *Power Systems, IEEE Transactions on*, 11(1):83 –92, February 1996.

[81] H.M. Khodr, J. Martinez-Crespo, M.A. Matos, and J. Pereira. Distribution systems reconfiguration based on OPF using Benders decomposition. *Power Delivery, IEEE Transactions on*, 24(4):2166 –2176, 2009.

[82] Sunyoung Kim and Masakazu Kojima. Exact solutions of some nonconvex quadratic optimization problems via SDP and SOCP relaxations. *Computational Optimization and Applications*, 26:143–154, 2003.

[83] Prabha Kundur. *Power system stability and control.* McGraw-Hill Professional, 1994.

[84] Kevin Lang and Satish Rao. Finding near-optimal cuts: an empirical evaluation. In *Proceedings of the fourth annual ACM-SIAM Symposium on Discrete algorithms*, SODA '93, pages 212–221, Philadelphia, PA, USA, 1993. Society for Industrial and Applied Mathematics.

[85] J. B. Lasserre. Global optimization with polynomials and the problem of moments. *SIAM J. on Optimization*, 11(3):796–817, 2000.

[86] J. B. Lasserre. Semidefinite programming vs. LP relaxations for polynomial programming. *Mathematics of Operations Research*, 27(2):347–360, 2002.

[87] Jean B. Lasserre. Polynomial programming: LP-relaxations also converge. *SIAM Journal on Optimization*, 15(2):383–393, 2005.

[88] G. Latorre, R.D. Cruz, J.M. Areiza, and A. Villegas. Classification of publications and models on transmission expansion planning. *Power Systems, IEEE Transactions on*, 18(2):938 – 946, May 2003.

[89] J. Lavaei and S. H. Low. Convexification of the optimal power flow problem. In *Proc. Allerton Conf. on Communication, Control, and Computing*, 2010.

[90] T. Leighton and S. Rao. Multicommodity max-flow min-cut theorems and their use in designing approximation algorithms. *J. ACM*, 46(6):787–832, 1999.

[91] E. J. Lerner. What's wrong with the electric grid? *Industrial Physicist*, 9(5):8–13, Oct. 2003.

[92] B.C. Lesieutre and I.A. Hiskens. Convexity of the set of feasible injections and revenue adequacy in FTR markets. *Power Systems, IEEE Transactions on*, 20(4):1790 – 1798, Nov. 2005.

[93] Miguel Sousa Lobo, Lieven Vandenberghe, Stephen Boyd, and Herv Lebret. Applications of second-order cone programming. *Linear Algebra and its Applications*, 284:193–228, Nov. 1998.

[94] L. Lovász and A. Schrijver. Cones of matrices and set-functions and 0–1 optimization. *SIAM Journal on Optimization*, 1(2):166–190, 1991.

[95] T. L. Magnanti and R. T. Wong. Network Design and Transportation Planning: Models and Algorithms. *Transportation Science*, 18(1):1–55, 1984.

[96] Probability methods subcommittee. IEEE reliability test system. *Power Apparatus and Systems, IEEE Transactions on*, 98(6):2047 –2054, Nov. 1979.

[97] Bojan Mohar. Isoperimetric numbers of graphs. *Journal of Combinatorial Theory, Series B*, 47(3):274 – 291, 1989.

[98] R. J. Muirhead. *Aspects of multivariate statistical theory.* Wiley, New York, New York, 1982.

[99] A. Y. Ng, M. I. Jordan, and Y. Weiss. On spectral clustering: Analysis and an algorithm. In *Advances in Neural Information Processing Systems 14*, pages 849–856. MIT Press, 2001.

[100] Pablo A. Parrilo. *Structured Semidefinite Programs and Semialgebraic Geometry Methods in Robustness and Optimization.* PhD thesis, Pasadena, CA, 2000.

[101] Pablo A. Parrilo and Bernd Sturmfels. Minimizing polynomial functions. In *Algorithmic and Quantitative Aspects of Real Algebraic Geometry in Mathematics and Computer Science*, pages 83–100, 2001.

[102] Mukund R. Patel. *Wind and solar power systems: design, analysis, and operation.* CRC Press, 2006.

[103] M.V.F. Pereira and N.J. Balu. Composite generation/transmission reliability evaluation. *Proceedings of the IEEE*, 80(4):470 –491, Apr. 1992.

[104] A. Prekopa and E. Boros. On the existence of a feasible flow in a stochastic transportation network. *Operations Research*, 39(1):119–129, 1991.

[105] I. J. Ramirez-Rosado and J. L. Bernal-Agustin. Reliability and costs optimization for distribution networks expansion using an evolutionary algorithm. *Power Engineering Review, IEEE*, 21(4):70–70, April 2001.

[106] M.J. Rider, A.V. Garcia, and R. Romero. Power system transmission network expansion planning using AC model. *Generation, Transmission Distribution, IET*, 1(5):731 –742, September 2007.

[107] R. Romero, A. Monticelli, A. Garcia, and S. Haffner. Test systems and mathematical models for transmission network expansion planning. *IEE Proceedings - Generation, Transmission and Distribution*, 149(1):27–36, 2002.

[108] Alexander Schrijver. *Theory of Linear and Integer Programming.* John Wiley & Sons, June 1998.

[109] Fred C. Schweppe, Michael C. Caramanis, Richard D. Tabors, and Roger E. Bohn. *Spot pricing of electricity.* Kluwer Academic Publishers, Boston, MA, 1988.

[110] A. Sharifnia and H. Z. Aashtiani. Transmission network planning: A method for synthesis of minimum-cost secure networks. *Power Apparatus and Systems, IEEE Transactions on*, PAS-104(8):2025–2034, August 1985.

[111] H. D. Sherali and C. H. Tuncbilek. A global optimization algorithm for polynomial programming problems using a reformulation-linearization technique. *Journal of Global Optimization*, 2:101–112, 1992.

[112] Hanif D. Sherali and Warren P. Adams. A hierarchy of relaxations between the continuous and convex hull representations for zero-one programming problems. *SIAM Journal on Discrete Mathematics*, 3(3):411–430, 1990.

[113] D. Shirmohammadi and H.W. Hong. Reconfiguration of electric distribution networks for resistive line losses reduction. *Power Delivery, IEEE Transactions on*, 4(2):1492 –1498, apr 1989.

[114] David B. Shmoys. *Cut problems and their application to divide-and-conquer*, pages 192–235. PWS Publishing Co., Boston, MA, USA, 1997.

[115] D. A. Spielman and S.-H. Teng. Spectral partitioning works: Planar graphs and finite element meshes. *Linear Algebra and its Applications*, 421(2-3):284 – 305, 2007. Special Issue in honor of Miroslav Fiedler.

[116] G. W. Stewart and J.-G. Sun. *Matrix Perturbation Theory (Computer Science and Scientific Computing)*. Academic Press, 1990.

[117] Jos F. Sturm. Using SeDuMi 1.02, a MATLAB toolbox for optimization over symmetric cones, 1999.

[118] L. Vandenberghe and S. Boyd. Semidefinite programming. *SIAM Review*, 38(1):49–95, 1996.

[119] Vijay V. Vazirani. *Approximation Algorithms*. Springer, March 2004.

[120] Juan Pablo Vielma, Shabbir Ahmed, and George L. Nemhauser. A lifted linear programming branch-and-bound algorithm for mixed-integer conic quadratic programs. *INFORMS J. on Computing*, 20:438–450, July 2008.

[121] R. Villasana. *Transmission network planning: A method for synthesis of minimum cost secure networks.* PhD thesis, Troy, NY, 1984.

[122] J. H. Wilkinson. *The Algebraic Eigenvalue Problem (Numerical Mathematics and Scientific Computation).* Oxford University Press, USA, April 1988.

[123] H. L. Willis. *Distributed Power Generation: Planning and Evaluation.* CRC Press, 2000.

[124] A. J. Wood and B. F. Wollenberg. *Power generation, operation, and control.* Knovel, second edition, 1996.

[125] Felix Wu, Pravin Varaiya, Pablo Spiller, and Shmuel Oren. Folk theorems on transmission access: Proofs and counterexamples. *Journal of Regulatory Economics*, 10:5–23, 1996.

[126] Tong Wu, M. Rothleder, Z. Alaywan, and A.D. Papalexopoulos. Pricing energy and ancillary services in integrated market systems by an optimal power flow. *Power Systems, IEEE Transactions on*, 19(1):339 – 347, Feb. 2004.

[127] H. Yoshida, K. Kawata, Y. Fukuyama, S. Takayama, and Y. Nakanishi. A particle swarm optimization for reactive power and voltage control considering voltage security assessment. *Power Systems, IEEE Transactions on*, 15(4):1232 –1239, November 2000.

[128] E.L. Zivi. Integrated shipboard power and automation control challenge problem. In *Power Engineering Society Summer Meeting, 2002 IEEE*, volume 1, pages 325 –330 vol.1, 2002.